
A PIPELINE FOR ENABLING PATH-SPECIFIC CAUSAL FAIRNESS IN OBSERVATIONAL HEALTH DATA

A PREPRINT

Aparajita Kashyap

Department of Biomedical Informatics
Columbia University
New York, NY, USA
ak4885@cumc.columbia.edu

Sara Matijevic

Big Data Institute
University of Oxford
Oxford, UK
sm6088@cumc.columbia.edu

Noémie Elhadad

Department of Biomedical Informatics
Columbia University
New York, NY, USA
noemie.elhadad@columbia.edu

Steven A. Kushner

Department of Psychiatry
Columbia University
New York, NY, USA
sk2602@cumc.columbia.edu

Shalmali Joshi

Department of Biomedical Informatics
Columbia University
New York, NY, USA
sj3261@cumc.columbia.edu

January 21, 2026

ABSTRACT

When training machine learning (ML) models for potential deployment in a healthcare setting, it is essential to ensure that they do not replicate or exacerbate existing healthcare biases. Although many definitions of fairness exist, we focus on *path-specific causal fairness*, which allows us to better consider the social and medical contexts in which biases occur (e.g., direct discrimination by a clinician or model versus bias due to differential access to the healthcare system) and to characterize how these biases may appear in learned models. In this work, we map the structural fairness model to the observational healthcare setting and create a generalizable pipeline for training causally fair models¹. The pipeline explicitly considers specific healthcare context and disparities to define a target "fair" model. Our work fills two major gaps: first, we expand on characterizations of the "fairness-accuracy" tradeoff by detangling direct and indirect sources of bias and jointly presenting these fairness considerations alongside considerations of accuracy in the context of broadly known biases. Second, we demonstrate how a foundation model trained without fairness constraints on observational health data can be leveraged to generate causally fair downstream predictions in tasks with known social and medical disparities. This work presents a model-agnostic pipeline for training causally fair machine learning models that address both direct and indirect forms of healthcare bias.

Keywords Causal fairness · foundation models · causal inference · observational health data · fair machine learning

¹Code available at https://github.com/reAIM-Lab/causal_fairness_health_pipeline

1 Introduction

The need for fairness in machine learning (ML) is well-documented, particularly in the context of healthcare, where there are known systemic disparities that can lead to bias in data collection and in downstream ML models [Chen et al., 2021]. Bias in the healthcare system exists through several avenues: implicit biases held by clinicians can directly lead to the lower quality of patient care [FitzGerald and Hurst, 2017], and inequitable exposures to social and environmental factors (e.g., environmental toxicants) can indirectly cause disparities in health outcomes [Bellavia et al., 2018]. Additionally, disparities in access and trust in the healthcare system can lead to disparities in healthcare utilization [Manuel, 2018]. Differences in healthcare utilization can impact the completeness of observational health data in particular, as these data are only collected when individuals access healthcare services [Sullivan et al., 2019]. We argue that, when training and evaluating data-driven models for potential use in healthcare settings, these different "avenues" of bias must be characterized in a case-specific manner that accounts for known healthcare disparities in the specific disease domain.

Many notions of fairness exist in machine learning [Gao et al., 2025]. Group fairness is defined by splitting a population into groups based on some sensitive attribute(s) and enforcing equal model performance across subgroups according to some metric(s). However, notions of group fairness are limited by assumptions about the underlying data (e.g., demographic parity assumes equal rates of positive outcomes across all groups) and by the conflicting nature of group fairness metrics that can render simultaneous enforcement impossible [Chouldechova, 2017]. Individual fairness defines a similarity metric and seeks to ensure that individuals defined as "similar" by this metric have similar outcomes under the model Dwork et al. [2012]. However, individual fairness is susceptible to biased data and can overlook difficult-to-capture socioeconomic privileges and disparities in resource allocation [Braverman, 2014]. Causal fairness looks to identify and mitigate "unfair" causal pathways between some characteristic(s) and the outcome. Causal fairness approaches allow users to compare bias in the data to bias in the model, which is not possible when evaluating disparities based on subgroup comparison of model performance metrics. However, causal fairness can be limited by the need for domain knowledge to identify the underlying causal structure of the data and the need for statistical identifiability to estimate causal effects from observational data [Pearl, 2000, Makhlof et al., 2024]. Additionally, calculating counterfactual quantities in high dimensions can be complex and unstable [Mitra et al., 2022].

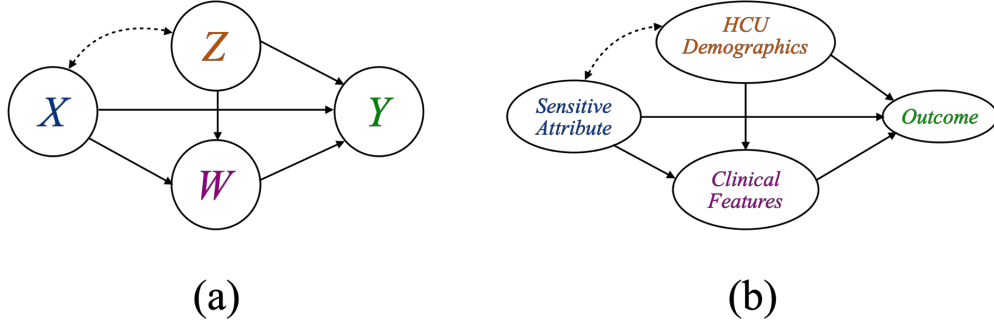


Figure 1: Standard Fairness Model: (a) Overview of SFM as presented in Plečko and Bareinboim [2024] (b) Clinically motivated mapping of SFM for observational health data

Figure 2: Causal directed acyclic graphs illustrating the standard fairness model and its mapping to observational health data, showing relationships between sensitive attributes, clinical features, healthcare utilization, and outcome

We argue that evaluation of fairness in healthcare should rely on *path-specific causal fairness*, which defines biased causal paths in the data-generating mechanism and seeks to ensure that the model does not replicate or introduce bias through these "unfair" causal pathways. We focus on path-specific causal fairness over other methods, such as counterfactual fairness Kusner et al. [2017] because path-specific causal fairness allows us to decompose the biases in the healthcare system and form hypotheses about specific social and medical disparities that a model may be replicating. Our work builds on the structural fairness model (SFM) defined in Plečko and Bareinboim [2024], which allows us to cluster variables into four groups (Figure 2a): sensitive attribute (X), outcome (Y), confounding variables (Z), and mediators (W). Through this clustering, we can ignore the relationships between variables within each cluster while maintaining identifiability of the relevant causal effects [Anand et al., 2023]. We offer a generalizable mapping of high-dimensional observational health data onto the SFM (Section 3.2, Figure 2b), eliminating the need for domain knowledge of the case-specific causal system.

We establish a pipeline for enforcing and evaluating path-specific causal fairness in clinical risk prediction models. Users can select target effects for fairness interventions and explore a more multidimensional fairness-accuracy tradeoff that

decomposes "bias" into specific paths that echo known health disparities. We demonstrate the pipeline's generalizability by applying it to four case studies. This generalizability is important given the rise of structured electronic health record (EHR) foundation models for healthcare Pang et al. [2025], which require adaptable methods for models that may not be trained to explicitly address fairness. Three of our cases (acute myocardial infarction, systemic lupus erythematosus, type 2 diabetes mellitus) leverage embeddings from a structured EHR foundation model Wornow et al. [2025] to train the baseline model on which fairness interventions are applied. Our fourth case (schizophrenia risk prediction) is built on a task-specific model to demonstrate the utility of our pipeline on a more "conventional" ML model.

Our contributions are as follows:

1. We offer a generalizable, clinically motivated mapping of tabular observational health data (e.g., EHR, administrative claims) onto the structural fairness model for framing clinical risk prediction problems.
2. We demonstrate the utility of dimensionality reduction methods to reduce the estimation error of doubly-robust path-specific causal effects.
3. We establish a pipeline for "diagnosing", enforcing, and evaluating path-specific causal fairness by contextualizing data-driven insights with known healthcare disparities
4. We demonstrate that there are no universally applicable causal or non-causal fairness interventions that provide optimal accuracy-causal fairness tradeoffs and illustrate the importance of testing naive, feature selection-based fairness interventions alongside known causal regularization strategies.
5. We expand on prior work characterizing fairness-accuracy tradeoffs and present a more comprehensive set of tradeoffs between accuracy and *path-specific* fairness, demonstrating the importance of context-specific prioritization of causal pathways.

2 Related Work

2.1 Enforcing causal fairness in machine learning

Training causally fair models is an open challenge in machine learning. To train counterfactually fair models, Kusner et al. [2017] propose limiting a model to learn only from features that are non-descendants of the sensitive attribute; however, this technique is not feasible in observational health data, where most clinical variables could be causal descendants of the sensitive attribute [Gopal et al., 2021, Meidert et al., 2023, Vohra-Gupta et al., 2023]. Counterfactual fairness is also enforced using learned representations that are invariant or orthogonal to the sensitive attribute Quinza et al. [2024], Chen and Zhu [2025] or through counterfactual data augmentation [Ma et al., 2023, Zhou et al., 2025, Robertson et al., 2025].

To enforce causal fairness with respect to path-specific measures, Plečko and Bareinboim [2024] present an in-processing regularization to penalize causal effects along specific paths in the structural fairness model (SFM) and enforce fair decision-making [Plečko and Bareinboim, 2023]. Other work develops interventions to reduce only the direct effect Stefano et al. [2020] or the effect of spurious features [Wang et al., 2021b]. Optimal transport has also been used to learn causally fair models [De Lara et al., 2024, Bayer et al., 2023, Nabi and Shpitser, 2018]. In particular, Nabi et al. [2019] propose to learn fair policies by sampling data from a 'debiased' data-generating process. A full review of causality-based methods for fair ML can be found in Su et al. [2022]. We compare path-specific in-processing and causally fair resampling to naive feature selection methods for their potential to reduce path-specific effects and find that methods specifically designed to address causal fairness do not universally outperform naive methods, even when fairness is evaluated using path-specific causal effects.

2.2 Navigating the "fairness-accuracy tradeoff"

Fairness and accuracy are important but potentially conflicting desiderata within ML Gittens et al. [2022], with many works conceptualizing this tradeoff as a Pareto frontier Valdivia et al. [2021], Wang et al. [2021a], Xu and Strohmer [2023]. Prior work in causality has aimed to measure this tradeoff, including by quantifying the extent to which model loss increases when trained under causal fairness constraints Plečko and Bareinboim [2025] and by using the "average treatment effect" to assess the impact of fairness interventions Ji et al. [2024]. However, the assumption that fairness and accuracy must exist as a "tradeoff" may be due to a lack of consideration of social and historical context [Wang et al., 2021a], limitations of the mathematical notations used to model fairness, and measurement error in biased data [Dutta et al., 2020]. Our work explicitly considers social context and baseline bias in the observational data by accounting for non-direct causal effects, as observational health data is known to reflect the biases of our medical system. For a more in-depth treatment of the necessity of the fairness-accuracy tradeoff, we refer readers to Li and Li [2025]. We

emphasize the importance of using path-specific causal fairness to assess ML models in the healthcare setting, breaking down bias into direct, indirect, and spurious causal effects. This allows us to consider the model in the context of broader health disparities, quantify the extent to which a learned model replicates and/or exacerbates unfair causal paths in the data, and measure the impact of fairness interventions on model performance.

2.3 Fairness in foundation models

Most work around fairness in foundation models focuses on language models [Wang et al., 2025, Gallegos et al., 2024] and vision models [Ali et al., 2023a]. In medical imaging specifically, prior work found significant subgroup performance differences in segmentation foundation models Li et al. [2024], Jin et al. [2024]. Other work echoes these findings and addresses these differences using balanced fine-tuning datasets Khan et al. [2023] or "fair PCA post-processing" Ali et al. [2023b]. Consistent with broader ethical ML literature Chen et al. [2021], Queiroz et al. [2025] discusses the ways that bias mitigation for medical vision foundation models must be an integrated effort involving investment at all steps in the AI pipeline, from data collection to training methodologies to deployment and regulation. Relatively little work focuses on fairness in tabular foundation models. Robertson et al. [2025] demonstrates how training on causally fair synthetic data can improve the fairness of tabular foundation models. In the case of in-context learning, Kenfack et al. [2025] illustrates the promise of pre-processing fairness methods. Our work examines the path-specific causal fairness of structured (tabular) EHR foundation models, both at the pretraining step and after linear probing, which has received little attention in prior work.

3 Preliminaries

3.1 Standard Fairness Model

The standard fairness model (SFM) [Plečko and Bareinboim, 2024] is a structural causal model (SCM) to assess causal fairness. An SCM [Pearl, 2000] is a formalized model of a data-generating process that defines the causal relationship between each of the variables in the system. The SFM defines the sensitive attribute (X) that can directly impact the outcome (Y). Additionally, X affects Y through a set of mediator variables (W), confounded by Z (Figure 2a). One key aspect of the SFM is the identifiability of the natural direct effect (NDE), natural indirect effect (NIE), and spurious effect (SE) from observational data. That is, under the assumption that the data-generating mechanism follows the SFM, all three effects can be estimated as nested counterfactuals from observational data (Appendix 9).

3.2 Clinical mapping of Standard Fairness Model

We leverage the SFM to define a generalizable procedure for mapping high-dimensional observational health data (e.g., EHRs, administrative claims) onto the SFM, thus providing a principled template for evaluating fairness in observational health settings. Such a generalizable mapping is important because relying on clinical domain knowledge to define structural assumptions is infeasible in high dimensions. Our mapping (Figure 2b) is as follows: as with the SFM, X remains the sensitive attribute and Y is the clinical outcome of interest. W represents a high-dimensional representation of a person's clinical record that can include information derived from diagnoses, medications, procedures, devices, laboratory tests, etc. These features can be derived directly from a person's clinical record or can be a learned representation of the clinical data presented as a set of embedding vectors. Finally, Z represents other demographic variables, baseline comorbidities known before a visit, if available, and **healthcare utilization**. Healthcare utilization (HCU) refers to the frequency, types, and patterns of healthcare services that an individual uses. HCU can serve as a proxy for several unobserved variables such as social determinants of health (typically constituting latent common causes between X and Z), including access to and trust in the healthcare system. In our work, we operationalize healthcare utilization as the frequency of visits. The NDE represents the "direct" effect of the sensitive attribute on the outcome; the NIE represents the effect of the sensitive attribute on the outcome as mediated by the rest of a person's observational health record (W). The SE represents the baseline change in the outcome distribution as a result of the two interventions $x = 0$ and $x = 1$ compared to their observational counterparts.

4 Methods

In Figure 3, we present a workflow for operationalizing the clinically motivated mapping of the SFM on a given problem that uses observational health data: i) define the task and key variables; ii) robustly estimate the path-specific causal effects; iii) train a baseline model; iv) select target effects (e.g., NDE, NIE, SE, some combination) for which to reduce disparities; v) perform and evaluate causal fairness enhancing interventions.

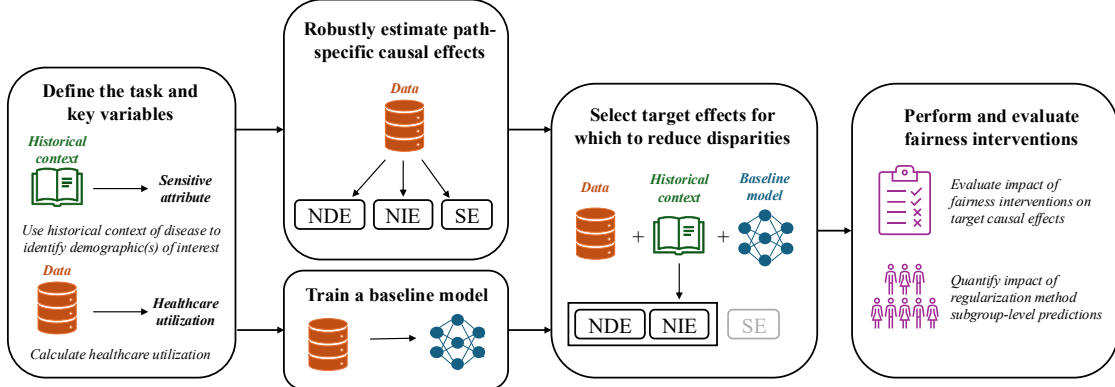


Figure 3: Overview of the proposed workflow. Starting with task selection, we outline the steps required to train and evaluate a causally fair model. In particular, we find that data-driven decision making must be combined with known historical context about healthcare disparities specific to the clinical task at hand.

Figure 4: Flowchart presenting the workflow outlined in this paper. The steps are: 1) define the task and key variables (in particular, select the sensitive attribute and calculate healthcare utilization); 2) robustly estimate the path-specific causal effects; 3) train a baseline model; 4) select target effects (e.g., NDE, NIE, SE, some combination) for which to reduce disparities; 5) perform and evaluate causal fairness enhancing interventions.

4.1 Define the task and key variables

Once a clinical prediction task is selected, we use this to set our outcome (Y) in the SFM. The sensitive attribute (X), however, still requires definition. X is typically a discrete variable, often binary, for which we want to measure and enforce path-specific fairness. While purely data-driven analysis based on all known sensitive attributes is important, it is often more crucial and feasible to assess how broadly known disparities reflect in the data and downstream learned models. We advocate for selecting a sensitive attribute that is associated with known (or hypothesized) disparities in broader health literature. We use race or gender as our main sensitive attributes for each case; however, selecting subgroups for X using an intersection of identities is possible under statistical feasibility (sufficient sample sizes to robustly evaluate path-specific effects). The next key variable(s), often ignored, are related to healthcare utilization. Healthcare utilization patterns drive predictive performance of learned models [Zink et al., 2024, Pang et al., 2025] and serve as noisy proxies for unobserved social drivers of health. We define healthcare utilization as the number of visits per year. If there is consistent information about the visit setting (e.g., outpatient, inpatient, pharmacy), we create separate healthcare utilization features for each visit setting. These healthcare utilization features, in combination with any "non-sensitive" demographic features, comprise the confounder set of the SFM (Z). Z must also include baseline health status, such as known comorbidities known at the beginning of the visit or stay, if data samples represent visits or stays. The clinical features (W) include all features used by the model that are not encapsulated by X , Z , and Y .

4.2 Robustly estimate path-specific causal effects

Given the systemic nature of medical disparities and typical mechanisms these propagate, we argue that fairness should be evaluated using path-specific causal effects. These effects must be characterized in both the raw observational data and in learned models to assess the relative change in causal fairness. Steps iii) and iv), therefore, require robust estimation of the NDE, NIE, and SE from finite observational samples under current practice (raw data), a trained baseline model ($f : X, Z, W \mapsto Y$), and any trained model that includes a fairness intervention [Jung et al., 2021, Plečko and Bareinboim, 2024].

Despite progress in doubly robust estimators, the dimensionality of W and Z remains a statistical bottleneck for finite sample estimators. We therefore assess the robustness of dimensionality reduction methods that provide the best tradeoff for robust path-specific estimation using synthetic data, where true effect sizes are known. We set the causal graph underlying the data-generating process to the SFM (Figure 2a) and initialize a different MLP to simulate each edge of the graph. We simulate synthetic data with dimensionality that closely matches the real data, with general function mappings (such as highly non-linear MLPs) to ensure that chosen dimensionality reduction will provide analogous robust estimates in real data where the ground-truth is unknown. Synthetic experiments show that doubly robust estimation alone still leads to large measurement errors in high dimensions (≥ 500 features) for the NDE and NIE

(Figure 9). We empirically evaluate methods of dimensionality reduction to identify the method(s) that lead to the most accurate path-specific effect estimates. Doubly robust estimators are effective because they only require one set of models (either the propensity models or outcome models) to be correctly specified [Li and Shen \[2020\]](#). Thus, we focus on dimensionality reduction methods that seek to retain predictive power about the sensitive attribute X or Y . For each method listed below, we test reduction to 20%, 40%, 50%, 60%, and 80% of the original dimensionality $|W|$.

- **Learn X :** We retain predictive power about X by identifying the subset of features in W that demonstrate a distribution shift between $X = 0$ and $X = 1$ (i.e., select features with the largest shift in mean difference between the $X = 0$ and $X = 1$ subpopulations).
- **Learn Y :** We retain predictive power in Y by identifying the "most important" subset of mediating features W for predicting the outcome Y . We examine importance through LASSO logistic regression, commonly used for genetic mediation analysis [Jérolon et al. \[2024\]](#), [Ye et al. \[2021\]](#). Additionally, we train an XGBoost-based outcome model and identify features through permutation feature importance (PFI) [Fisher et al. \[2019\]](#), a model-agnostic measure of feature importance.
- **Learn W :** While not directly supported by doubly robust theory, we test the impact of learning a condensed representation of W that minimizes reconstruction loss. For this, we train a two-layer MLP autoencoder to generate a lower-dimensional embedding of W .

4.3 Train a baseline model

The baseline model is trained on all variables in X , W , and Z . Our pipeline is model-agnostic, so any model architecture can be used. The evaluation of causal effects on model output requires "hard" (binary) labels; we create these labels by selecting the threshold probability that jointly optimizes sensitivity and specificity in the validation dataset.

4.4 Select target effects for which to reduce disparities

Once we select a clinical problem and establish a baseline model, we should select the causal paths to prioritize for elimination. This idea of prioritizing causal pathways is similar to the notion of "business necessity" [Plečko and Bareinboim \[2024\]](#); however, rather than ignoring bias through specific pathways, we recognize that regularization across all causal pathways may not be feasible while maintaining model performance ("no free lunch"). Thus, we advocate for case-specific prioritization of causal pathways that accounts for domain knowledge of health disparities and relative disparities in the data compared to baseline models. We examine 1) the relative sizes of each causal effect in the raw data and the ways in which each observed causal effect may be reflective of known healthcare disparities in the specific clinical domain; 2) how causal effects may be exacerbated in the baseline model compared to the raw data; and 3) the contextual factors (either from health disparities literature or algorithmic fairness literature) that may explain the causal effects of the baseline model.

4.5 Perform and evaluate fairness interventions

Causal regularization is often proposed as an effective method to mitigate path-specific unfairness due to its ability to target individual or a combination of effects. Feature selection is a commonly used strategy for training model fairness over a range of fairness definitions [\[Belitz et al., 2021\]](#), [\[Galhotra et al., 2022\]](#), [\[Yang et al., 2023\]](#), [\[Njoku et al., 2025\]](#). Complementarily, non-causal regularization techniques that operationalize notions of group and individual fairness are prominent in algorithmic fairness literature. We evaluate the following **causal regularization** strategies:

- **Path-specific inprocessing:** We implement the path-specific inprocessing approach from [Plečko and Bareinboim \[2024\]](#). This approach leverages the model output for the true data and the counterfactual (changing a person's race or gender) to estimate the NDE, NIE, and SE. It then penalizes these effects in the loss function. We train models that regularize a single effect (NDE-only, NIE-only, SE-only) and models that regularize with respect to all three effects.
- **Causally fair resampling:** We implement a version of the approach from [Nabi et al. \[2019\]](#), which blocks unfair causal pathways by learning fair distributions over the sensitive attribute and mediator. The method computes path-specific effects using inverse probability weighting and employs constrained optimization to find model parameters that minimize the targeted path-specific effect. We average over the sensitive attribute and mediators using the learned fair distributions, thus removing the influence of the sensitive attribute through the targeted causal pathways.

We evaluate multiple **feature selection**-based strategies:

- **Demographic unawareness:** We train models without any explicit demographic information (race and gender), including the sensitive attribute. This experiment is representative of the idea of "fairness through unawareness", a simple but widely debated debiasing method in fair ML and ML for health [Höltgen and Oliver \[2025\]](#), [Basu \[2023\]](#).
- **"Unbiased" feature selection:** We identify "highly biased features" as those with a large standardized mean difference (SMD) between the specified sensitive attribute and remove these features during model training. For a specified feature count (n), we keep the n features with the lowest SMD.
- **Greedy feature selection** We greedily select features that maximize predictive performance while minimizing bias. We quantify a feature's contribution to predictive performance using a feature importance metric and quantify its contribution to bias using SMD, as defined above. The relative contribution of SMD to the feature score is selected based on the "elbow point" that maximizes distance from the baseline importance-SMD tradeoff.

Finally, we test the following **non-causal regularization** strategies:

- **Learning fair representations:** We investigate representations learned to optimize individual fairness model proposed in [Zemel et al. \[2013\]](#). This is a pre-processing method that seeks to learn a representation of the data that obscures information about the sensitive attribute while maintaining predictive power.
- **Equalized Odds:** We investigate the impact of imposing a group fairness constraint on path-specific causal fairness. Specifically, we operationalize equalized odds [Hardt et al. \[2016\]](#) by adding a regularization term to the loss function that penalizes differences in the true and false positive rates.

We evaluate the models based on performance (AUROC) and path-specific causal effects (focusing on the "prioritized" causal pathways, as described in Section 4.4). In order to better characterize the impact of the regularized prediction model on specific subgroups of patients, we also report the Pearson Correlation between the sensitive attribute and the true outcome, as well as between the sensitive attribute and the predicted outcomes (Appendix 12-15). This allows us to compare the relationship between the sensitive attribute and the outcome in the data, baseline model, and the "fair" model. This analysis is especially important for tasks where our goal is to improve racial fairness, as we report the causal effects with respect to Black vs. White patients, and assessing the impact on other racial groups is crucial.

5 Experiments and Results

We demonstrate our proposed workflow on four clinical risk prediction tasks: acute myocardial infarction (AMI), systemic lupus erythematosus (SLE), type 2 diabetes mellitus (T2DM), and schizophrenia (SCZ). We select these tasks because they span a diverse set of clinical domains and are all associated with known health disparities (Section 5.1). In each case, we select an "at-risk" cohort of individuals with related symptoms or comorbidities of the illness, and seek to predict which of these individuals will go on to develop the given disease. Our framing of tasks within the "at-risk" cohort rather than a general population increases the task difficulty because many well-established risk factors for the disease are widely present in the data and are therefore less predictive of the outcome of interest. This forces the model to rely less on risk factors that clinicians are already attuned to, thus increasing potential for clinical utility. For AMI, SLE, and T2DM, we use the phenotypes defined in a prior foundation model benchmark [Pang et al. \[2025\]](#) and retrain the LLAMA foundation model on CUMC-EHR. We select the LLAMA model because is a widely used architecture used both within and outside the healthcare setting [Wormow et al. \[2025\]](#).

5.1 Define the task and key variables

We demonstrate our pipeline in two datasets representing typical structured observational health data sources: CUMC-EHR, a deidentified EHR of \sim 5.3 million patients from a large urban academic medical center, and the deidentified Merative Multi-State Medicaid dataset (MDCD). The MDCD dataset includes all data collected from healthcare providers for medical billing for 25 million patients from 11 different US states. Both datasets are structured using the Observational Medical Outcomes Partnership Common Data Model [Hripcsak et al. \[2019\]](#), ensuring reproducibility in other compatible health datasets. In both datasets, gender is recorded as male or female and the method of capture for this variable (e.g., patient-reported, assigned at birth) is not recorded and may vary between patients. We are therefore unable to extend our analyses beyond binary gender. In CUMC-EHR, race is captured as a categorical variable: American Indian or Alaskan Native, Asian, Black, Native Hawaiian or Pacific Islander, White, Missing, and Other. In MDCD, race is captured with three categories: Black, White, and Missing. The method of capture for race is also unknown in both datasets.

5.1.1 Acute Myocardial Infarction (AMI)

We predict AMI in patients with prior ischemic heart disease. We focus on mitigating gender disparities ($x_0 = \text{female}$, $x_1 = \text{male}$) due to known gender-based differences in presenting symptoms that can lead to underdiagnosis and delayed diagnosis of AMI in women [Kim et al., 2023b, Ngaruiya et al., 2024, Imboden et al., 2026]. We predict AMI onset using the embeddings from a LLAMA foundation model Wornow et al. [2025] pre-trained on CUMC-EHR; the model uses RoPE embeddings to encode temporal information and is trained using next token prediction (NTP) with context length 8192. The model embeddings represent a person's clinical history (W) and can be optionally combined with X and Z to predict the downstream outcome. This dataset does not contain comprehensive information about visit settings; thus, we represent healthcare utilization as a single variable defined as the number of distinct days with clinical "touchpoints" (visits, diagnoses, or procedures) per year. Z consists of healthcare utilization and patient race.

5.1.2 Systemic Lupus Erythematosus (SLE)

We predict the first occurrence of SLE among individuals with at least one SLE-related symptom or a prescription of a drug used to treat SLE symptoms. We focus on mitigating gender disparities ($x_0 = \text{female}$, $x_1 = \text{male}$) in the case of SLE due to differing diagnosis rates (4 – 22% of diagnosed SLE patients are male) and significantly differing symptom profiles across sexes Tan et al. [2012], do Socorro Teixeira Moreira Almeida et al. [2011]. Additionally, prior experimental work has found that clinicians faced with otherwise identical symptom profiles are less likely to diagnose men with SLE Simard et al. [2022]. We use the same data source (CUMC-EHR), LLAMA model, and healthcare utilization as outlined above for AMI.

5.1.3 Type 2 Diabetes Mellitus (T2DM)

We predict T2DM onset from the at-risk cohort defined in Pang et al. [2025] and a validated diabetes phenotype definition [Suchard et al., 2021]. We focus on mitigating racial disparities ($x_0 = \text{White}$, $x_1 = \text{Black}$). T2DM is known to have a higher prevalence among Black individuals compared to White individuals, likely due to disparities in socioeconomic status that increase diabetes risk [Deng et al., 2025, Hackl et al., 2024]. In addition to racial differences in prevalence, we find that several rule-based clinical algorithms for quantifying diabetes risk appear to underestimate T2DM risk for Black individuals, likely due to the absence of social and economic determinants of health from these algorithms [Cronjé et al., 2023]. It is important to measure the extent to which ML-based clinical prediction algorithms may remedy or exacerbate the biases found in such non-ML clinical algorithms. We use CUMC-EHR, the LLAMA model, and the healthcare utilization calculation for task definition as outlined above. However, since our sensitive attribute is patient race, we include patient gender in Z .

5.1.4 Schizophrenia (SCZ)

For the case of SCZ risk prediction, our "at-risk" cohort is defined as individuals with at least 3 years of observation and at least one psychosis diagnosis, and we predict schizophrenia onset one year after the first psychosis visit. We mandated three years of observation because external validation of the SCZ phenotype demonstrates that requiring three years of prior observation improves the positive predictive value from 69% to 77% [Finnerty et al., 2024]. Black individuals are overdiagnosed with schizophrenia due to differences in the interpretation of affective symptoms Trierweiler et al. [2000], Gara et al. [2019]. Additionally, rates of SCZ diagnosis following psychosis are higher for Black individuals compared to white individuals Moe et al. [2024]. For these reasons, we focus on mitigating racial disparities ($x_0 = \text{White}$, $x_1 = \text{Black}$). The SCZ prediction model is trained for this single task using the MDCD data. We generated features (W) based on frequency of conditions, laboratory tests, procedures and duration of prescriptions. We define healthcare utilization through 10 setting-specific frequency variables (e.g., outpatient, inpatient). Z consists of healthcare utilization and patient gender.

5.2 Robustly estimate path-specific causal effects

Using synthetic data, we demonstrate that estimating causal effects in high mediator dimensions ($|W| \geq 500$) leads to large estimation errors in the NDE and NIE (Figure 9, Table 2). We test each of the dimensionality reduction methods outlined in Section 4.2 on various mediator dimension sizes, ranging from $|W| = 750$ to $|W| = 1,750$. We consistently find that dimensionality reduction methods that identify the most important features for predicting Y , particularly PFI, are most effective at reducing both the NDE and NIE estimation error across all sample sizes (Figure 5). The spurious effect calculation is not impacted by changing the representation of W . These results are broadly consistent for $|W| = 750$, $|W| = 1,000$ and $|W| = 1,500$ (Appendix 10). In the case of AMI, SLE, and T2DM, we learn the features most predictive of Y through PFI [Fisher et al., 2019], as this yields the best results in the experiments where $|W| = 750$ (and the clinical embeddings are all $|W| = 768$). In the case of SCZ, we select highly predictive features

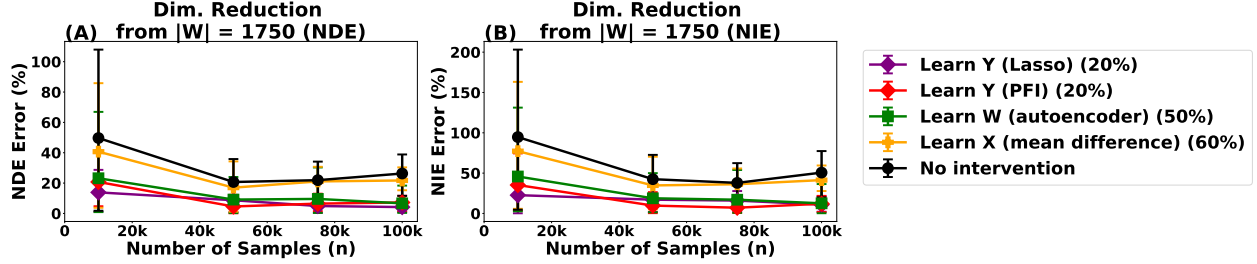


Figure 5: Error in the path-specific causal estimates for dimensionality $|W| = 1,750$. Each line corresponds to a different dimensionality reduction method, with the black line corresponding to no dimensionality reduction. The NDE estimation error is reflected in part (a), and the NIE estimation error is reflected in part (b). We find that interventions that identify features important for predicting the outcome (Y) outperform all other methods.

Figure 6: Side-by-side line plots with associated error bars. Each line is a different color, corresponding to the given legend of dimensionality reduction techniques

using augmented feature occlusion (AFO), a permutation analysis method appropriate for temporal models [Tonekaboni et al., 2020].

5.3 Train a baseline model

For the AMI, SLE, and T2DM prediction tasks, we pre-train a LLAMA model to generate embeddings (embedding dimension = 768) that represent a person’s clinical history. We use these embeddings, demographic features, and healthcare utilization information to train a logistic regression model as the baseline for each of these three tasks. We focus this approach rather than on finetuning the full foundation model due to its lower computational cost and relatively high performance [Pang et al., 2025]. For the SCZ prediction task, we employ a task-specific model: we bin data into 90-day increments and train an encoder-only transformer model using BCE loss.

Disease	NDE		NIE		SE	
	Data	Baseline model	Data	Baseline model	Data	Baseline model
AMI	0.003 (-0.003, 0.004)	0.073 (0.032, 0.077)	0.008 (0.005, 0.009)	0.153 (0.143, 0.157)	-0.001 (-0.001, -0.000)	-0.005 (-0.008, -0.004)
SLE	-0.002 (-0.002, -0.001)	-0.038 (-0.047, -0.025)	0.000 (-0.000, 0.000)	-0.012 (-0.021, -0.008)	0.000 (-0.000, 0.000)	-0.002 (-0.002, -0.001)
T2DM	0.014 (0.002, 0.016)	0.033 (0.027, 0.050)	0.005 (-0.004, 0.007)	0.059 (0.053, 0.107)	0.002 (0.000, 0.002)	0.003 (-0.015, 0.007)
SCZ	0.018 (0.005, 0.031)	0.120 (0.104, 0.134)	0.017 (0.003, 0.027)	0.015 (-0.000, 0.039)	-0.016 (-0.017, -0.012)	-0.069 (-0.073, -0.061)

Table 1: We report the Natural Direct Effect (NDE), Natural Indirect Effect (NIE), and Spurious Effect (SE) in the dataset and the baseline model for each prediction task. We report the effect size based on the held-out test set to remain consistent with the evaluation of model regularization methods and report accompanying 95% confidence intervals derived through bootstrapping.

5.4 Select target effects for which to reduce disparities

For each task, we report the path-specific causal effects for the raw data and baseline models in Table 1 and contextualize this information with known healthcare disparities to select which causal effects we aim to focus on.

5.4.1 Acute Myocardial Infarction (AMI)

When examining causal effects in the data, only the NIE is significant (0.008 [95% CI: 0.005, 0.009]); the positive value of the NIE indicates that an individual with clinical features drawn from a "male" population distribution is more likely to be diagnosed with AMI. This is consistent with findings that clinicians underdiagnose women with AMI due to a differing "typical" symptom profile [Kim et al., 2023b, Ngaruiya et al., 2024, Imboden et al., 2026]. In the baseline model, both the NDE and NIE increase by an order of magnitude (NDE: 0.073; NIE: 0.153), while the SE remains relatively small (−0.005 [−0.008, −0.004]). The increase in NDE and NIE indicates that the model introduces direct bias against women that does not exist in the dataset, and that the model is more tuned to a "classically male" symptom profile for AMI compared to clinical practice. We therefore focus on jointly reducing the NDE and NIE for AMI risk prediction.

5.4.2 Systemic Lupus Erythematosus (SLE)

When examining the impact of gender on SLE, the NIE and SE are insignificant, and the NDE is small ($-0.002 [-0.002, -0.001]$). The NDE and NIE increase significantly in the baseline model (NDE: $-0.038 [-0.047, -0.025]$; NIE: $-0.012 [-0.021, -0.008]$), with the NDE increasing more than the NIE. The negative NDE indicates that women are more likely to be diagnosed than men, consistent with the low diagnosis rates of SLE in men [Tan et al., 2012, Simard et al., 2022]. The NIE suggests that individuals with a "male" distribution are more likely to be diagnosed with SLE than individuals with data drawn from a "female" distribution. Due to direct bias against men when diagnosing SLE and the larger size of the NDE in both the data and the baseline model, we focus on reducing the NDE for SLE.

5.4.3 Type 2 Diabetes Mellitus (T2DM)

In the T2DM cohort, the dataset reflects a significant NDE ($0.014 [0.002, 0.016]$) that indicates overdiagnosis of T2DM in Black individuals, consistent with epidemiological literature [Deng et al., 2025, Hackl et al., 2024]. The NDE is exacerbated in the baseline model ($0.033 [0.027, 0.134]$), which also worsens the NIE ($0.059 [0.053, 0.107]$). The NIE suggests that an individual with clinical features drawn from a "white" population distribution is more likely to be diagnosed with T2DM; this is consistent with known algorithmic biases [Cronjé et al., 2023]. The SE remains insignificant in the data and baseline model. Thus, we focus on jointly reducing the NDE and NIE for T2DM risk prediction.

5.4.4 Schizophrenia (SCZ)

The NDE, NIE, and SE are all similar in magnitude (NDE: $0.018 [0.005, 0.031]$; NIE: $0.017 [0.003, 0.027]$; SE: $-0.016 [-0.017, -0.012]$) in the data. The positive NDE is reflective of overdiagnosis of SCZ in Black patients compared to white patients, while the positive NIE is reflective of the fact that an individual with clinical features drawn from a "white" population distribution is more likely to be diagnosed with SCZ. The negative SE suggests that the confounder variables in Z (gender, healthcare utilization) may play a larger role in diagnosis for Black patients than white patients. Of these three effects, the NDE reflects known overdiagnosis of SCZ in Black individuals [Trierweiler et al., 2000], while the NIE and SE may reflect broader disparities in quality of care [Fiscella and Sanders, 2016] and healthcare utilization [Manuel 2018], respectively. In the baseline model, we observe a significant exacerbation in NDE (Model: $0.120 [0.104, 0.134]$) and SE (Model: $-0.069 [-0.073, -0.061]$). The NIE remains similar the data ($0.015 [0, 0.039]$). These causal effects suggest that the model is more reliant on race than a clinician might be (NDE), and that the disparate weight on confounding variables (healthcare utilization, gender) is more pronounced in the model than in clinical practice (SE). Based on the tenfold increase in NDE between the raw data and the baseline model and the known problems with overdiagnosis of schizophrenia in Black individuals, we prioritize reducing the NDE in the SCZ risk prediction case. Additionally, we treat reduction of SE as a secondary target, as the effect may be due to disparities in healthcare utilization.

5.5 Perform and evaluate fairness interventions

We discuss the efficacy and impact of all interventions outlined in Section 4.5 for each clinical prediction task. We present the AUROC-effect tradeoff for each of the "target" effects (Figure 7).

5.5.1 Acute Myocardial Infarction (AMI)

As shown in Figure 7A and 7E, the baseline model and demographic-unaware model are associated with the highest model performance (Baseline AUROC: $0.812 [0.796, 0.825]$; demographic unawareness: $0.814 [0.799, 0.832]$). However, both models have large NDE (> 0.05) and NIE (> 0.14). Causally fair resampling maintains near-equal performance to the baseline model ($0.809 [0.794, 0.825]$) while eliminating the NDE; however, the NIE is still relatively large ($-0.111 [0.095, 0.115]$). Greedy feature selection also eliminates the NDE and improves the NIE beyond the baseline and causally fair resampling ($0.074 [0.069, 0.087]$); however, there is a 6.8% drop in AUROC ($0.757 [0.738, 0.777]$). If we allow model performance to drop even further, the "unbiased" feature selection intervention (AUROC: $0.695 [0.674, 0.716]$) reduces the NIE even further ($0.027 [0.021, 0.046]$) while eliminating the NDE. Through this, we observe that it is possible to eliminate the NDE without sacrificing model performance, but there is a clear tradeoff between reducing the NIE and maintaining model performance (Appendix 12).

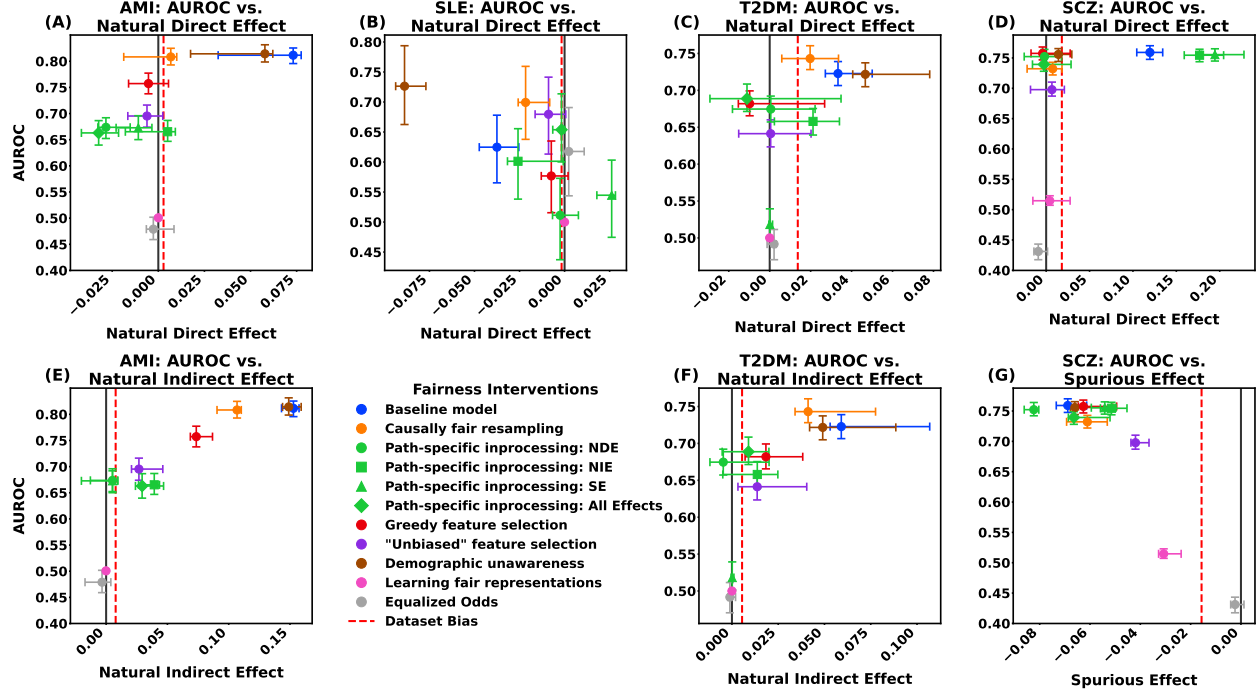


Figure 7: Tradeoffs between model performance and target path-specific effects across all tasks. We plot the target path-specific effects for each intervention (NDE, NIE, and/or SE) against the model performance (AUROC) for each of the "target" effects (Section 4.4). (A) and (E) show the NDE and NIE for AMI; (B) shows the NDE for SLE; (C) and (F) show the NDE and NIE for T2DM; (D) and (G) show the NDE and SE for SCZ.

Figure 8: 4 columns by 2 rows of scatter plots. Points are colored differently based on the fairness intervention (included in the legend) and have associated error bars. The x-axis is the path-specific causal effect and the y-axis shows AUROC.

5.5.2 Systemic Lupus Erythematosus (SLE)

As shown in Figure 7B, the demographic-unaware model is associated with the best AUROC (0.726 [0.662, 0.794]). However, the NDE ($-0.089 [-0.094, -0.077]$) is significantly higher compared to the data and the baseline model. The next-best model performances (outperforming even the baseline model) are associated with causally fair resampling (0.699 [0.638, 0.759]) and selection of "unbiased" features (0.680 [0.613, 0.741]). The causally fair resampling reduces, but does not eliminate the NDE ($-0.030 [-0.044, -0.030]$) and "unbiased" feature selection eliminates the NDE (Appendix 13).

5.5.3 Type 2 Diabetes Mellitus (T2DM)

The highest performing model that eliminates both the NDE (Figure 7C) and NIE (Figure 7F) is the one trained using path-specific in-processing. The AUROC of this model (0.689 [0.671, 0.709]) represents a 7.3% drop in performance relative to the highest-performing model, which uses the causally fair resampling intervention (AUROC: 0.743 [0.728, 0.760]). However, causally fair resampling maintains a significant NDE (0.020 [0.006, 0.034]) or the NIE (0.041 [0.034, 0.078]). Thus, we observe a tradeoff between model performance and model bias along both the NDE and NIE (Appendix 14).

5.5.4 Schizophrenia (SCZ)

As shown in Figure 7D and 7G, the baseline model is associated with the best performance (AUROC: 0.759 [0.748, 0.770]) but larger NDE and SE compared to the data (NDE: 0.120 [0.104, 0.134]; SE: $-0.069 [-0.073, -0.061]$). Greedy feature selection maintains the performance of the baseline model (AUROC: 0.758 [0.747, 0.768]) while eliminating the NDE and maintaining a similar SE to the baseline model ($-0.063 [-0.065, 0.049]$). If we allow for deterioration in performance, we find that "unbiased" feature selection (AUROC: 0.698 [0.687, 0.710]) eliminates the NDE and reduces the SE to $-0.042 [-0.044, -0.037]$. Thus, while

we do not observe a tradeoff between performance and NDE, we do observe a tradeoff between performance and SE (Appendix 15).

6 Discussion

Our pipeline enables the following insights on enabling fairness-enhancing interventions in observational health data.

Mapping observational health data to the SFM enables generalizable evaluation of causal fairness. Our mapping can be used for multiple clinical risk prediction problems and works with clinical variables (W) generated directly from the data and with feature embeddings generated through foundation models. This addresses known problems in causality, including the need for domain-specific knowledge when constructing a causal graph and ensuring identifiability of the relevant path-specific effects [Makhlof et al., 2024]. We also account for a known limitation in fair ML literature more broadly, where data are abstracted from the societal context in which they exist [Selbst et al., 2019, Singh et al., 2024]: by integrating domain-specific disparities knowledge, we can ensure that interventions target known problems within the clinical context.

Causal effect estimation in high dimensions requires dimensionality reduction via outcome-driven feature selection. The underpinning of this fairness pipeline is the ability to robustly estimate path-specific causal effects in high dimensions of W , as the dimensionality of the clinical representation (W) may vary from hundreds (AMI, SLE, T2DM) to over 1000 (SCZ). We leverage state-of-the-art doubly robust estimators, which allow for incorrect specification of either the propensity models or the outcome models, and find that for high-dimensional W , estimation error is significantly reduced by selecting features based on their predictive power with respect to Y , consistent with mediation analyses in high-throughput data [Jérolon et al., 2024, Chén et al., 2018]. In the case where Z were to be a high-dimensional vector, approaches related to high-dimensional propensity analysis could help ensure robust estimates Brookhart et al. [2006], Schneeweiss et al. [2009], Zhang et al. [2022].

Models not explicitly trained for fairness unpredictably introduce causal unfairness. Across all four cases, we observed a significant increase in the NDE between the dataset and the baseline model (no fairness intervention). The magnitude of the increase varies greatly by task: the NDE increases by factors ranging from 2.4 (T2DM) to 24 (AMI), and the NIE and SE differences between the data and model vary similarly. This result reinforces the importance of context-specific prioritization of causal effects: in addition to identifying the causal pathways through which bias surfaces in the data and the pathways where the causal effects are exacerbated in the baseline model relative to the data, considering the existing healthcare context is essential. This prioritization is also important given the observed tradeoffs between specific causal pathways and model performance. Addressing such known limitations of existing clinical risk algorithms may increase the potential for future clinical utility [Chakradeo et al., 2025].

Consider causal and feature selection-based fairness interventions for reducing path-specific causal effects. We test interventions from different types of fairness literature, including group fairness (equalized odds [Hardt et al., 2016]), individual fairness (learning fair representations [Zemel et al., 2013]), and causal fairness (path-specific inprocessing [Plečko and Bareinboim, 2024], causal resampling [Nabi et al., 2019]). Additionally, we test several naive feature selection approaches not designed to target any specific type of fairness (fairness through unawareness [Höltgen and Oliver, 2025], selection of unbiased features, greedy feature selection). No universally optimal approach exists. Interestingly, we find that causal methods do not always have the best efficacy; relatively naive feature selection approaches, including greedy feature selection and selecting "unbiased" features, can significantly improve causal fairness. We hypothesize that naive feature selection may be a feasible approach in observational health data due to some interdependence between features: even if the "most biased" features are removed from the model, the patterns that underlie a person's health are still learnable from other features in the data. We additionally find that non-causal algorithmic fairness interventions (e.g., methods that target individual [Zemel et al., 2013] and group [Hardt et al., 2016] fairness objectives) are unable to maintain reasonable model performance when targeting the systemic disparities prevalent in healthcare. These results illustrate the importance of implementing the full pipeline (Figure 3) and trying both causal and non-causal interventions to mitigate path-specific causal effects.

Limitations and future work: We focus on single-attribute fairness tasks. Intersectional fairness approaches may be appropriate for diseases where multiple axes of disparities (e.g., race, gender) are known [Kim et al., 2023a, Islek et al., 2025]; however, this would require larger datasets with more diverse populations. In the case of T2DM and SCZ, we measure the path-specific effects by comparing White and Black populations; however, both datasets include at least one other race group. While individuals from these groups are included in all models and in the correlation analysis, we do not explicitly model disparities in these other race groups as well. Future work should consider fairness across non-binary categorical variables. Finally, our work explores *tradeoffs* between path-specific causal biases and model performance. While we provide guidance on how to decide which causal pathways to target for bias mitigation, further discussion with clinical experts would be required to select the best model for a given task.

7 Conclusion

In this work, we establish a pipeline for operationalizing path-specific causal fairness in clinical prediction tasks. We define a generalizable mapping of tabular observational health data onto the structural fairness model, and demonstrate how to construct this mapping in the context of known health disparities. We illustrate the importance of defining model fairness through causal pathways that replicate real-world disparity and quantify the extent to which learned models exacerbate these existing biases. By characterizing a more comprehensive fairness-accuracy tradeoff that examines multiple fairness pathways alongside accuracy, we illustrate the importance of context-specific prioritization and enforcement of causal pathways over which a model should be "fair". While our work focuses on the algorithms in the healthcare setting, several components of the pipeline (robust estimation of causal effects, selection of causal pathways to target for bias mitigation, trial of causal and non-causal fairness interventions) are applicable to fair ML outside of healthcare.

8 Endmatter

Ethical Considerations: This study was approved by the relevant institutional review board (IRB). Informed consent was waived by the IRB due to low risk to subject welfare and logistical infeasibility of contacting millions of patients from a de-identified database.

Generative AI usage statement: No AI tools were used to generate text for this manuscript. The authors used generative AI (Gemini 3) to assist with coding (graphing, formatting of tables) and manuscript editing (proofreading, grammar). All generative AI outputs were verified by the authors.

References

Junaid Ali, Matthäus Kleindessner, Florian Wenzel, Kailash Budhathoki, Volkan Cevher, and Chris Russell. Evaluating the fairness of discriminative foundation models in computer vision. In *Proceedings of the 2023 AAAI/ACM Conference on AI, Ethics, and Society*, pages 809–833, New York, NY, USA, August 2023a. ACM.

Junaid Ali, Matthäus Kleindessner, Florian Wenzel, Kailash Budhathoki, Volkan Cevher, and Chris Russell. Evaluating the fairness of discriminative foundation models in computer vision. In *Proceedings of the 2023 AAAI/ACM Conference on AI, Ethics, and Society*, AIES '23, page 809–833, New York, NY, USA, 2023b. Association for Computing Machinery. ISBN 9798400702310. doi:[10.1145/3600211.3604720](https://doi.org/10.1145/3600211.3604720). URL <https://doi.org/10.1145/3600211.3604720>.

Tara V Anand, Adele H Ribeiro, Jin Tian, and Elias Bareinboim. Causal effect identification in cluster DAGs. *Proc. Conf. AAAI Artif. Intell.*, 37(10):12172–12179, June 2023.

Anirban Basu. Use of race in clinical algorithms. *Science Advances*, 9(21):eadd2704, May 2023. doi:[10.1126/sciadv.add2704](https://doi.org/10.1126/sciadv.add2704). URL <https://www.science.org/doi/10.1126/sciadv.add2704>. Publisher: American Association for the Advancement of Science.

Fritz Bayer, Drago Plecko, Niko Beerenwinkel, and Jack Kuipers. Fair Clustering: A Causal Perspective, December 2023. URL <http://arxiv.org/abs/2312.09061>. arXiv:2312.09061 [stat].

Clara Belitz, Lan Jiang, and Nigel Bosch. Automating procedurally fair feature selection in machine learning. In *Proceedings of the 2021 AAAI/ACM Conference on AI, Ethics, and Society*, AIES '21, page 379–389, New York, NY, USA, 2021. Association for Computing Machinery. ISBN 9781450384735. doi:[10.1145/3461702.3462585](https://doi.org/10.1145/3461702.3462585). URL <https://doi.org/10.1145/3461702.3462585>.

Andrea Bellavia, Ami R Zota, Linda Valeri, and Tamarra James-Todd. Multiple mediators approach to study environmental chemicals as determinants of health disparities. *Environ. Epidemiol.*, 2(2):e015, June 2018.

Paula Braveman. What are health disparities and health equity? we need to be clear. *Public Health Rep.*, 129 Suppl 2 (1_suppl2):5–8, January 2014.

M. Alan Brookhart, Sebastian Schneeweiss, Kenneth J. Rothman, Robert J. Glynn, Jerry Avorn, and Til Stürmer. Variable selection for propensity score models. *American Journal of Epidemiology*, 163(12):1149–1156, June 2006. ISSN 0002-9262. doi:[10.1093/aje/kwj149](https://doi.org/10.1093/aje/kwj149).

Kaustubh Chakradeo, Inchuen Huynh, Sedrah B Balaganeshan, Ole L Dollerup, Hjørdis Gade-Jørgensen, Susanne K Laupstad, Mikkel Malham, Tri-Long Nguyen, Adam Hulman, and Tibor V Varga. Navigating fairness aspects of clinical prediction models. *BMC Med.*, 23(1):567, October 2025.

Irene Y Chen, Emma Pierson, Sherri Rose, Shalmali Joshi, Kadija Ferryman, and Marzyeh Ghassemi. Ethical machine learning in healthcare. *Annual Review of Biomedical Data Science*, 4:123–144, May 2021. doi:<https://doi.org/10.1146/annurev-biodatasci-092820-114757>. URL <https://www.annualreviews.org/content/journals/10.1146/annurev-biodatasci-092820-114757>.

Shuyi Chen and Shixiang Zhu. Counterfactual Fairness Through Transforming Data Orthogonal to Bias. In *Proceedings of the 31st ACM SIGKDD Conference on Knowledge Discovery and Data Mining* V.2, KDD '25, pages 239–249, New York, NY, USA, August 2025. Association for Computing Machinery. ISBN 9798400714542. doi:[10.1145/3711896.3736895](https://doi.org/10.1145/3711896.3736895). URL <https://dl.acm.org/doi/10.1145/3711896.3736895>.

Alexandra Chouldechova. Fair prediction with disparate impact: A study of bias in recidivism prediction instruments. *Big Data*, 5(2):153–163, June 2017.

Oliver Y Chén, Ciprian Crainiceanu, Elizabeth L Ogburn, Brian S Caffo, Tor D Wager, and Martin A Lindquist. High-dimensional multivariate mediation with application to neuroimaging data. *Biostatistics (Oxford, England)*, 19(2):121–136, April 2018. ISSN 1465-4644. doi:[10.1093/biostatistics/kxx027](https://doi.org/10.1093/biostatistics/kxx027). URL <https://www.ncbi.nlm.nih.gov/pmc/articles/PMC5862274/>.

Hélène T Cronjé, Alexandros Katsiferis, Leonie K Elsenburg, Thea O Andersen, Naja H Rod, Tri-Long Nguyen, and Tibor V Varga. Assessing racial bias in type 2 diabetes risk prediction algorithms. *PLOS Glob. Public Health*, 3(5):e0001556, May 2023.

Lucas De Lara, Alberto González-Sanz, Nicholas Asher, Laurent Risser, and Jean-Michel Loubes. Transport-based counterfactual models. *J. Mach. Learn. Res.*, 25(1):136:6512–136:6570, January 2024. ISSN 1532-4435.

Yangyang Deng, Mohammad Moniruzzaman, Breanna Rogers, Lu Hu, Ram Jagannathan, and Kosuke Tamura. Unveiling inequalities: Racial, ethnic, and socioeconomic disparities in diabetes: Findings from the 2007–2020 NHANES data among U.S. adults. *Prev. Med. Rep.*, 50(102957):102957, February 2025.

Maria do Socorro Teixeira Moreira Almeida, Josué da Costa Arcoverde, Mário Nicolau Barros Jacobino, and Antônio Rodrigues Coimbra Neto. Male systemic lupus erythematosus, an overlooked diagnosis. *Clin. Pract.*, 1(4):e103, September 2011.

Sanghamitra Dutta, Dennis Wei, Hazar Yueksel, Pin-Yu Chen, Sijia Liu, and Kush R. Varshney. Is there a trade-off between fairness and accuracy? a perspective using mismatched hypothesis testing. In *Proceedings of the 37th International Conference on Machine Learning*, ICML'20, Virtual Conference, 2020. JMLR.org.

Cynthia Dwork, Moritz Hardt, Toniann Pitassi, Omer Reingold, and Richard Zemel. Fairness through awareness. In *Proceedings of the 3rd Innovations in Theoretical Computer Science Conference*, ITCS '12, pages 214–226, New York, NY, USA, January 2012. Association for Computing Machinery. ISBN 978-1-4503-1115-1. doi:[10.1145/2090236.2090255](https://doi.org/10.1145/2090236.2090255). URL <https://dl.acm.org/doi/10.1145/2090236.2090255>.

Molly T. Finnerty, Atif Khan, Kai You, Rui Wang, Gyojeong Gu, Deborah Layman, Qingxian Chen, Noémie Elhadad, Shalmali Joshi, Paul S. Appelbaum, Todd Lencz, Sander Markx, Steven A. Kushner, and Andrey Rzhetsky. Prevalence and incidence measures for schizophrenia among commercial health insurance and medicaid enrollees. *Schizophrenia*, 10(1):68, August 2024. ISSN 2754-6993. doi:[10.1038/s41537-024-00490-0](https://doi.org/10.1038/s41537-024-00490-0). URL <https://www.nature.com/articles/s41537-024-00490-0>. Publisher: Nature Publishing Group.

Kevin Fiscella and Mechelle R Sanders. Racial and ethnic disparities in the quality of health care. *Annu. Rev. Public Health*, 37(1):375–394, January 2016.

Aaron Fisher, Cynthia Rudin, and Francesca Dominici. All Models are Wrong, but Many are Useful: Learning a Variable's Importance by Studying an Entire Class of Prediction Models Simultaneously. *Journal of Machine Learning Research*, 20(177):1–81, 2019. ISSN 1533-7928. URL <http://jmlr.org/papers/v20/18-760.html>.

Chloë Fitzgerald and Samia Hurst. Implicit bias in healthcare professionals: a systematic review. *BMC Med. Ethics*, 18(1):19, March 2017.

Sainyam Galhotra, Karthikeyan Shanmugam, Prasanna Sattigeri, and Kush R. Varshney. Causal feature selection for algorithmic fairness. In *Proceedings of the 2022 International Conference on Management of Data*, SIGMOD '22, page 276–285, New York, NY, USA, 2022. Association for Computing Machinery. ISBN 9781450392495. doi:[10.1145/3514221.3517909](https://doi.org/10.1145/3514221.3517909). URL <https://doi.org/10.1145/3514221.3517909>.

Isabel O. Gallegos, Ryan A. Rossi, Joe Barrow, Md Mehrab Tanjim, Sungchul Kim, Franck Dernoncourt, Tong Yu, Ruiyi Zhang, and Nesreen K. Ahmed. Bias and fairness in large language models: A survey. *Computational Linguistics*, 50(3):1097–1179, September 2024. doi:[10.1162/coli_a_00524](https://doi.org/10.1162/coli_a_00524). URL <https://aclanthology.org/2024.cl-3.8/>.

Jianhui Gao, Benson Chou, Zachary R. McCaw, Hilary Thurston, Paul Varghese, Chuan Hong, and Jessica Gronsbell. What Is Fair? Defining Fairness in Machine Learning for Health. *Statistics in Medicine*, 44(20-22):e70234, September 2025. ISSN 0277-6715. doi:[10.1002/sim.70234](https://doi.org/10.1002/sim.70234). URL <https://pmc.ncbi.nlm.nih.gov/articles/PMC12436242/>.

Michael A Gara, Shula Minsky, Steven M Silverstein, Theresa Miskimen, and Stephen M Strakowski. A naturalistic study of racial disparities in diagnoses at an outpatient behavioral health clinic. *Psychiatr. Serv.*, 70(2):130–134, February 2019.

Alex Gittens, Bülent Yener, and Moti Yung. An adversarial perspective on accuracy, robustness, fairness, and privacy: Multilateral-tradeoffs in trustworthy ml. *IEEE Access*, 10:120850–120865, 2022. doi:[10.1109/ACCESS.2022.3218715](https://doi.org/10.1109/ACCESS.2022.3218715).

Dipesh P Gopal, Ula Chetty, Patrick O'Donnell, Camille Gajria, and Jodie Blackadder-Weinstein. Implicit bias in healthcare: clinical practice, research and decision making. *Future Healthc. J.*, 8(1):40–48, March 2021.

Caitlin M Hackl, Wei-Chen Lee, Hanaa S Sallam, Hani Jneid, Kendall M Campbell, and Hani Serag. Racial disparities in selected complications and comorbidities among people with type 2 diabetes. *Healthcare (Basel)*, 12(8):846, April 2024.

Moritz Hardt, Eric Price, and Nathan Srebro. Equality of opportunity in supervised learning. In *Proceedings of the 30th International Conference on Neural Information Processing Systems*, NIPS'16, page 3323–3331, Red Hook, NY, USA, 2016. Curran Associates Inc. ISBN 9781510838819.

Benedikt Höltgen and Nuria Oliver. Reconsidering fairness through unawareness from the perspective of model multiplicity. In *Proceedings of the 5th ACM Conference on Equity and Access in Algorithms, Mechanisms, and Optimization*, EAAMO '25, page 241–255, New York, NY, USA, 2025. Association for Computing Machinery. ISBN 9798400721403. doi:[10.1145/3757887.3763007](https://doi.org/10.1145/3757887.3763007). URL <https://doi.org/10.1145/3757887.3763007>.

George Hripcak, Ning Shang, Peggy L Peissig, Luke V Rasmussen, Cong Liu, Barbara Benoit, Robert J Carroll, David S Carrell, Joshua C Denny, Ozan Dikilitas, Vivian S Gainer, Kayla Marie Howell, Jeffrey G Klann, Iftikhar J Kullo, Todd Lingren, Frank D Mentch, Shawn N Murphy, Karthik Natarajan, Jennifer A Pacheco, Wei-Qi Wei, Ken Wiley, and Chunhua Weng. Facilitating phenotype transfer using a common data model. *J. Biomed. Inform.*, 96(103253):103253, August 2019.

Mary T Imboden, Erin Koltner, Jane H Bryant, Adrienne Jones, Renee C Swanson, Lori M Tam, and Kevin J Woolf. Sex disparities in acute myocardial infarction diagnosis and treatment. *Am. J. Cardiol.*, 259:179–186, January 2026.

Duygu Islek, Alvaro Alonso, Wayne Rosamond, Anna Kucharska-Newton, Yejin Mok, Kunihiro Matsushita, Silvia Koton, Michael Joseph Blaha, and Viola Vaccarino. Racial differences in recurrent acute myocardial infarction: Findings from the ARIC cohort. *J. Am. Heart Assoc.*, 15(1):e040133, December 2025.

Zhenlan Ji, Pingchuan Ma, Shuai Wang, and Yanhui Li. Causality-aided trade-off analysis for machine learning fairness. In *Proceedings of the 38th IEEE/ACM International Conference on Automated Software Engineering*, ASE '23, page 371–383, Echternach, Luxembourg, 2024. IEEE Press. ISBN 9798350329964. doi:[10.1109/ASE56229.2023.00105](https://doi.org/10.1109/ASE56229.2023.00105). URL <https://doi.org/10.1109/ASE56229.2023.00105>.

Ruinan Jin, Zikang Xu, Yuan Zhong, Qingsong Yao, Qi Dou, S. Kevin Zhou, and Xiaoxiao Li. Fairmedfm: fairness benchmarking for medical imaging foundation models. In *Proceedings of the 38th International Conference on Neural Information Processing Systems*, NIPS '24, Red Hook, NY, USA, 2024. Curran Associates Inc. ISBN 9798331314385.

Yonghan Jung, Jin Tian, and Elias Bareinboim. Estimating identifiable causal effects through double machine learning. *Proc. Conf. AAAI Artif. Intell.*, 35(13):12113–12122, May 2021.

Allan Jérolon, Flora Alarcon, Florence Pittion, Magali Richard, Olivier François, Etienne E. Birmelé, and Vittorio Perduca. Group lasso based selection for high-dimensional mediation analysis, September 2024. URL [http://arxiv.org/abs/2409.20036](https://arxiv.org/abs/2409.20036). arXiv:2409.20036 [q-bio].

Patrik Kenfack, Samira Ebrahimi Kahou, and Ulrich Aivodji. Towards fair in-context learning with tabular foundation models, 2025. URL <https://arxiv.org/abs/2505.09503>.

Muhammad Osama Khan, Muhammad Muneeb Afzal, Shujaat Mirza, and Yi Fang. How fair are medical imaging foundation models? In Stefan Hegselmann, Antonio Parziale, Divya Shanmugam, Shengpu Tang, Mercy Nyamewaa Asiedu, Serina Chang, Tom Hartvigsen, and Harvineet Singh, editors, *Proceedings of the 3rd Machine Learning for Health Symposium*, volume 225 of *Proceedings of Machine Learning Research*, pages 217–231, San Diego, CA, 10 Dec 2023. PMLR. URL <https://proceedings.mlr.press/v225/khan23a.html>.

So Ree Kim, Sunga Bae, Ji Yoon Lee, Min Sun Kim, Mi-Na Kim, Wook-Jin Chung, Jang-Ho Bae, Juneyoung Lee, and Seong-Mi Park. Gender disparities in prevalence by diagnostic criteria, treatment and mortality of newly diagnosed acute myocardial infarction in korean adults. *Sci. Rep.*, 13(1):4120, March 2023a.

So Ree Kim, Sunga Bae, Ji Yoon Lee, Min Sun Kim, Mi-Na Kim, Wook-Jin Chung, Jang-Ho Bae, Juneyoung Lee, and Seong-Mi Park. Gender disparities in prevalence by diagnostic criteria, treatment and mortality of newly diagnosed acute myocardial infarction in korean adults. *Sci. Rep.*, 13(1):4120, March 2023b.

Matt Kusner, Joshua Loftus, Chris Russell, and Ricardo Silva. Counterfactual fairness. In *Proceedings of the 31st International Conference on Neural Information Processing Systems*, NIPS'17, pages 4069–4079, Red Hook, NY, USA, December 2017. Curran Associates Inc. ISBN 978-1-5108-6096-4.

Jingyang Li and Guoqiang Li. Triangular trade-off between robustness, accuracy, and fairness in deep neural networks: A survey. *ACM Comput. Surv.*, 57(6), February 2025. ISSN 0360-0300. doi:10.1145/3645088. URL <https://doi.org/10.1145/3645088>.

Qing Li, Yizhe Zhang, Yan Li, Jun Lyu, Meng Liu, Longyu Sun, Mengting Sun, Qirong Li, Wenyue Mao, Xinran Wu, Yajing Zhang, Yinghua Chu, Shuo Wang, and Chengyan Wang. An Empirical Study on the Fairness of Foundation Models for Multi-Organ Image Segmentation. In *proceedings of Medical Image Computing and Computer Assisted Intervention – MICCAI 2024*, volume LNCS 15012, pages 432–442, Marrakesh, Morocco, October 2024. Springer Nature Switzerland.

Xiaochun Li and Changyu Shen. Doubly robust estimation of causal effect: Upping the odds of getting the right answers. *Circ Cardiovasc Qual Outcomes*, 13:e006065, Jan 2020. doi:10.1161/CIRCOUTCOMES.119.006065. URL <https://pubmed.ncbi.nlm.nih.gov/31888348/>.

Jing Ma, Ruocheng Guo, Aidong Zhang, and Jundong Li. Learning for Counterfactual Fairness from Observational Data. In *Proceedings of the 29th ACM SIGKDD Conference on Knowledge Discovery and Data Mining*, KDD '23, pages 1620–1630, New York, NY, USA, August 2023. Association for Computing Machinery. ISBN 9798400701030. doi:10.1145/3580305.3599408. URL <https://dl.acm.org/doi/10.1145/3580305.3599408>.

Karima Makhlouf, Sami Zhioua, and Catuscia Palamidessi. When causality meets fairness: A survey. *J. Log. Algebr. Methods Program.*, 141(101000):101000, October 2024.

Jennifer I Manuel. Racial/ethnic and gender disparities in health care use and access. *Health Serv. Res.*, 53(3): 1407–1429, June 2018.

Ursula Meidert, Godela Dönniges, Thomas Bucher, Frank Wieber, and Andreas Gerber-Grote. Unconscious bias among health professionals: A scoping review. *Int. J. Environ. Res. Public Health*, 20(16):6569, August 2023.

Nandita Mitra, Jason Roy, and Dylan Small. The future of causal inference. *Am. J. Epidemiol.*, 191(10):1671–1676, September 2022.

Aubrey M Moe, Elyse Llamocca, Heather M Wastler, Danielle L Steelesmith, Guy Brock, Oladunni Oluwoye, and Cynthia A Fontanella. Racial and ethnic disparities in the diagnosis and early treatment of first-episode psychosis. *Schizophr. Bull. Open*, 5(1):sgae019, January 2024.

Razieh Nabi and Ilya Shpitser. Fair Inference on Outcomes. *Proceedings of the ... AAAI Conference on Artificial Intelligence. AAAI Conference on Artificial Intelligence*, 2018:1931–1940, February 2018. ISSN 2159-5399. URL <https://pmc.ncbi.nlm.nih.gov/articles/PMC5963284/>.

Razieh Nabi, Daniel Malinsky, and Ilya Shpitser. Learning Optimal Fair Policies. *Proceedings of machine learning research*, 97:4674–4682, June 2019. ISSN 2640-3498. URL <https://pmc.ncbi.nlm.nih.gov/articles/PMC6935348/>.

Christine Ngaruiya, Zainab Samad, Salma Tajuddin, Zarmeen Nasim, Rebecca Leff, Awais Farhad, Kyle Pires, Muhammad Alamgir Khan, Lauren Hartz, and Basmah Safdar. Identification of gender differences in acute myocardial infarction presentation and management at aga khan university Hospital-Pakistan: Natural language processing application in a dataset of patients with cardiovascular disease. *JMIR Form. Res.*, 8:e42774, December 2024.

Uchechukwu F Njoku, Alberto Abelló, Besim Bilalli, and Gianluca Bontempi. Towards fair machine learning using many-objective feature selection. *Appl. Soft Comput.*, 181(113411):113411, September 2025.

Chao Pang, Vincent Jeanselme, Young Sang Choi, Xinzhuo Jiang, Zilin Jing, Aparajita Kashyap, Yuta Kobayashi, Yanwei Li, Florent Pollet, Karthik Natarajan, and Shalmali Joshi. Fomoh: A clinically meaningful foundation model evaluation for structured electronic health records, 2025. URL <https://arxiv.org/abs/2505.16941>.

Judea Pearl. *Causality: Models, Reasoning, and Inference*. Cambridge University Press, New York, NY, 2000. ISBN 0-521-77362-8.

Drago Plecko and Elias Bareinboim. Causal fairness for outcome control. In *Proceedings of the 37th International Conference on Neural Information Processing Systems*, NIPS '23, pages 47575–47597, Red Hook, NY, USA, December 2023. Curran Associates Inc.

Drago Plecko and Elias Bareinboim. Fairness-accuracy trade-offs: a causal perspective. In *Proceedings of the Thirty-Ninth AAAI Conference on Artificial Intelligence and Thirty-Seventh Conference on Innovative Applications of Artificial Intelligence and Fifteenth Symposium on Educational Advances in Artificial Intelligence*, AAAI'25/IAAI'25/EAAI'25, Philadelphia, PA, 2025. AAAI Press. ISBN 978-1-57735-897-8. doi:10.1609/aaai.v39i25.34833. URL <https://doi.org/10.1609/aaai.v39i25.34833>.

Drago Plečko and Elias Bareinboim. Causal Fairness Analysis: A Causal Toolkit for Fair Machine Learning. *Foundations and Trends® in Machine Learning*, 17(3):304–589, January 2024. ISSN 1935-8237, 1935-8245. doi:10.1561/2200000106. URL <https://www.nowpublishers.com/article/Details/MAL-106>. Publisher: Now Publishers, Inc.

Dilermando Queiroz, Anderson Carlos, André Anjos, and Lilian Berton. Fair foundation models for medical image analysis: Challenges and perspectives, 2025. URL <https://arxiv.org/abs/2502.16841>.

Francesco Quinza, Cecilia Casolo, Krikamol Muandet, Yucen Luo, and Niki Kilbertus. Learning counterfactually invariant predictors, 2024. URL <https://arxiv.org/abs/2207.09768>.

Jake Robertson, Noah Hollmann, Samuel Müller, Noor Awad, and Frank Hutter. FairPFN: A tabular foundation model for causal fairness. In Aarti Singh, Maryam Fazel, Daniel Hsu, Simon Lacoste-Julien, Felix Berkenkamp, Tegan Maharaj, Kiri Wagstaff, and Jerry Zhu, editors, *Proceedings of the 42nd International Conference on Machine Learning*, volume 267 of *Proceedings of Machine Learning Research*, pages 51787–51808, San Diego, CA, 13–19 Jul 2025. PMLR. URL <https://proceedings.mlr.press/v267/robertson25a.html>.

Sebastian Schneeweiss, Jeremy A. Rassen, Robert J. Glynn, Jerry Avorn, Helen Mogun, and M. Alan Brookhart. High-dimensional propensity score adjustment in studies of treatment effects using health care claims data. *Epidemiology (Cambridge, Mass.)*, 20(4):512–522, July 2009. ISSN 1044-3983. doi:10.1097/EDE.0b013e3181a663cc. URL <https://www.ncbi.nlm.nih.gov/pmc/articles/PMC3077219/>.

Andrew D. Selbst, Danah Boyd, Sorelle A. Friedler, Suresh Venkatasubramanian, and Janet Vertesi. Fairness and abstraction in sociotechnical systems. In *Proceedings of the Conference on Fairness, Accountability, and Transparency*, FAT* ’19, page 59–68, New York, NY, USA, 2019. Association for Computing Machinery. ISBN 9781450361255. doi:10.1145/3287560.3287598. URL <https://doi.org/10.1145/3287560.3287598>.

Julia F Simard, Yashaar Chaichian, Nada Rizk, Amadeia Rector, Candace H Feldman, and Titilola O Falasinnu. Are we missing lupus in males? evidence of cognitive bias from a randomized experiment in the united states. *Am. J. Epidemiol.*, 191(1):230–233, January 2022.

Nimisha Singh, Amita Kapoor, and Neha Soni. A sociotechnical perspective for explicit unfairness mitigation techniques for algorithm fairness. *International Journal of Information Management Data Insights*, 4(2):100259, November 2024.

Pietro G. Di Stefano, James M. Hickey, and Vlasisos Vasileiou. Counterfactual fairness: removing direct effects through regularization, 2020.

Cong Su, Guoxian Yu, Jun Wang, Zhongmin Yan, and Lizhen Cui. A review of causality-based fairness machine learning. *Intelligence & Robotics*, 2(3):244–274, August 2022. ISSN ISSN 2770-3541 (Online). doi:10.20517/ir.2022.17. URL <https://www.oaepublish.com/articles/ir.2022.17>. Publisher: OAE Publishing Inc.

Marc A Suchard, Martijn J Schuemie, Harlan M Krumholz, Seoyoung C You, Ren Chen, Nicole Pratt, Christian Reich, Patrick Ryan, and George Hripcsak. Large-scale evidence generation and evaluation across a network of databases for type 2 diabetes mellitus (legend-t2dm): a protocol for a series of multinational, real-world comparative cardiovascular effectiveness and safety studies. *BMJ Open*, 11(1):e043247, 2021. doi:10.1136/bmjopen-2020-043247. URL <https://bmjopen.bmjjournals.org/content/11/1/e043247>.

Mackenzie W Sullivan, Fabian T Camacho, Anne M Mills, and Susan C Modesitt. Missing information in statewide and national cancer databases: Correlation with health risk factors, geographic disparities, and outcomes. *Gynecol. Oncol.*, 152(1):119–126, January 2019.

Tze Chin Tan, Hong Fang, Laurence S Magder, and Michelle A Petri. Differences between male and female systemic lupus erythematosus in a multiethnic population. *J. Rheumatol.*, 39(4):759–769, April 2012.

Sana Tonekaboni, Shalmali Joshi, Kieran R Campbell, David Duvenaud, and Anna Goldenberg. What went wrong and when? instance-wise feature importance for time-series black-box models. In *Proceedings of the 34th International Conference on Neural Information Processing Systems*, NIPS ’20, Red Hook, NY, USA, 2020. Curran Associates Inc. ISBN 9781713829546.

Steven J. Trierweiler, Harold W. Neighbors, Cheryl Munday, Estina E. Thompson, Victoria J. Binion, and John P. Gomez. Clinician attributions associated with the diagnosis of schizophrenia in African American and non-African American patients. *Journal of Consulting and Clinical Psychology*, 68:171–175, 2000. ISSN 1939-2117. doi:10.1037/0022-006X.68.1.171. Place: US Publisher: American Psychological Association.

Ana Valdivia, Javier Sánchez-Monedero, and Jorge Casillas. How fair can we go in machine learning? assessing the boundaries of accuracy and fairness. *International Journal of Intelligent Systems*, 36(4):1619–1643, 2021. doi:<https://doi.org/10.1002/int.22354>. URL <https://onlinelibrary.wiley.com/doi/abs/10.1002/int.22354>.

Shetal Vohra-Gupta, Liana Petruzzi, Casey Jones, and Catherine Cubbin. An intersectional approach to understanding barriers to healthcare for women. *J. Community Health*, 48(1):89–98, February 2023.

Yuyan Wang, Xuezhi Wang, Alex Beutel, Flavien Prost, Jilin Chen, and Ed H. Chi. Understanding and improving fairness-accuracy trade-offs in multi-task learning. In *Proceedings of the 27th ACM SIGKDD Conference on Knowledge Discovery & Data Mining*, KDD ’21, page 1748–1757, New York, NY, USA, 2021a. Association for Computing Machinery. ISBN 9781450383325. doi:[10.1145/3447548.3467326](https://doi.org/10.1145/3447548.3467326). URL <https://doi.org/10.1145/3447548.3467326>.

Zhao Wang, Kai Shu, and Aron Culotta. Enhancing model robustness and fairness with causality: A regularization approach. In Amir Feder, Katherine Keith, Emaad Manzoor, Reid Pryzant, Dhanya Sridhar, Zach Wood-Doughty, Jacob Eisenstein, Justin Grimmer, Roi Reichart, Molly Roberts, Uri Shalit, Brandon Stewart, Victor Veitch, and Diyi Yang, editors, *Proceedings of the First Workshop on Causal Inference and NLP*, pages 33–43, Punta Cana, Dominican Republic, November 2021b. Association for Computational Linguistics. doi:[10.18653/v1/2021.cinlp-1.3](https://doi.org/10.18653/v1/2021.cinlp-1.3). URL <https://aclanthology.org/2021.cinlp-1.3/>.

Zichong Wang, Avash Palikhe, Zhipeng Yin, and Wenbin Zhang. Fairness in language models: A tutorial. In *Proceedings of the 34th ACM International Conference on Information and Knowledge Management*, pages 6849–6852, New York, NY, USA, November 2025. ACM.

Michael Wornow, Suhana Bedi, Miguel Angel Fuentes Hernandez, Ethan Steinberg, Jason Alan Fries, Christopher Re, Sanmi Koyejo, and Nigam H. Shah. Context clues: Evaluating long context models for clinical prediction tasks on ehrs, 2025. URL <https://arxiv.org/abs/2412.16178>.

Shizhou Xu and Thomas Strohmer. Fair data representation for machine learning at the pareto frontier. *J. Mach. Learn. Res.*, 24(1), January 2023. ISSN 1532-4435.

Zhi Yang, Ziming Wang, Changwu Huang, and Xin Yao. An explainable feature selection approach for fair machine learning. In *Lecture Notes in Computer Science*, Lecture Notes in Computer Science, pages 75–86. Springer Nature Switzerland, Cham, 2023.

Zhaoxin Ye, Yeying Zhu, and Donna L Coffman. Variable selection for causal mediation analysis using LASSO-based methods. *Statistical Methods in Medical Research*, 30(6):1413–1427, June 2021. ISSN 0962-2802. doi:[10.1177/0962280221997505](https://doi.org/10.1177/0962280221997505). URL <https://www.ncbi.nlm.nih.gov/pmc/articles/PMC8189011/>.

Rich Zemel, Yu Wu, Kevin Swersky, Toni Pitassi, and Cynthia Dwork. Learning fair representations. In Sanjoy Dasgupta and David McAllester, editors, *Proceedings of the 30th International Conference on Machine Learning*, volume 28 of *Proceedings of Machine Learning Research*, pages 325–333, Atlanta, Georgia, USA, 17–19 Jun 2013. PMLR. URL <https://proceedings.mlr.press/v28/zemel13.html>.

Linying Zhang, Yixin Wang, Martijn J Schuemie, David M Blei, and George Hripcsak. Adjusting for indirectly measured confounding using large-scale propensity score. *J. Biomed. Inform.*, 134(104204):104204, October 2022.

Zeyu Zhou, Tianci Liu, Ruqi Bai, Jing Gao, Murat Kocaoglu, and David I. Inouye. Counterfactual fairness by combining factual and counterfactual predictions. In *Proceedings of the 38th International Conference on Neural Information Processing Systems*, volume 37 of *NIPS ’24*, pages 47876–47907, Red Hook, NY, USA, June 2025. Curran Associates Inc. ISBN 9798331314385.

Anna Zink, Hongzhou Luan, and Irene Y. Chen. Access to care improves ehr reliability and clinical risk prediction model performance, 2024. URL <https://arxiv.org/abs/2412.07712>.

9 Path-specific effects for fairness analysis

The natural direct effect (NDE) quantifies the impact of changing a person's sensitive attribute while keeping the effects through mediator variables (W) at the observed level. Consider the binary sensitive attribute $x \in \{0, 1\}$. Then, the direct effect of the sensitive attribute at baseline $x = 0$ is given by:

$$NDE_{x_0, x_1}(y) = P(y_{x_1, W_{x_0}}) - P(y_{x_0}) \quad (1)$$

The natural indirect effect (NIE) quantifies the change in the outcome distribution mediated through W only. Specifically, the NIE compares the outcome when the mediators' distribution is set to $x = 0$ to when the mediators are equal to the values they would be when $x = 1$:

$$NIE_{x_1, x_0}(y) = P(y_{x_1, W_{x_0}}) - P(y_{x_1}) \quad (2)$$

In the healthcare setting, distinguishing direct and indirect effects is crucial as the NDE effectively indicates a direct source of discrimination, distinct from the cumulative and broader bias in the healthcare system reflected in the individual's electronic health record (NIE).

Finally, the spurious effect (SE) quantifies the difference between the observational and the interventional outcome distribution. When calculating the NDE and NIE, we move to the interventional setting, where we set the sensitive attribute to $x = 0$ or $x = 1$ and "cut" the association between X and Z . The spurious effect captures the baseline change in the outcome distribution as a result of the two interventions $x = 0$ and $x = 1$ compared to their observational counterparts. Let,

$$ExpSE_{x_0}(y) := P(y|x=0) - P(y_{x_0}), \quad ExpSE_{x_1}(y) := P(y|x=1) - P(y_{x_1}) \quad (3)$$

The spurious effect is the difference between these two sub-effects, namely:

$$SE = ExpSE_{x_1}(y) - ExpSE_{x_0}(y) \quad (4)$$

Thus, a "fair" model with respect to the spurious effect would be one where severing the link between X and Z has the same impact on the outcome Y regardless of the value of X .

10 Robust estimation of path-specific causal effects in synthetic data

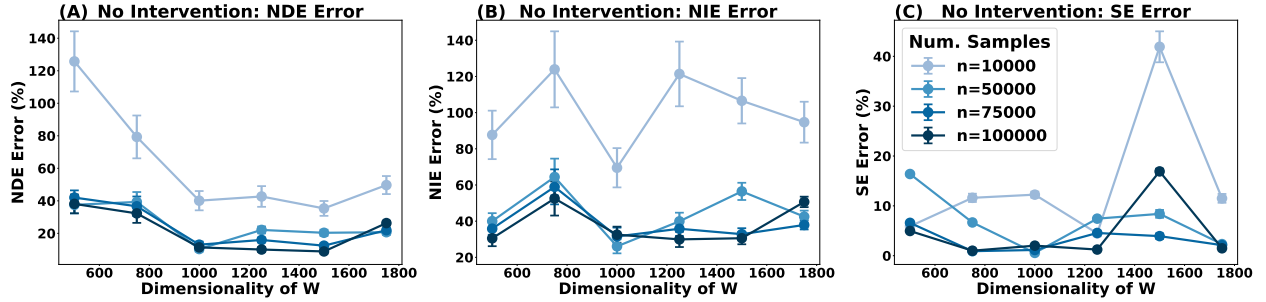


Figure 9: Error in the path-specific causal estimates for the (a) natural direct effect (NDE), (b) natural indirect effect (NIE), and (c) spurious effect (SE). Error is highest for a small sample size. The estimates are generated using doubly robust estimation, but still demonstrate large error for NDE and NIE.

Figure 10: Line graph with error bars showing the causal estimation error on the y-axis and the dimensionality of W on the x-axis.

We create synthetic data using the causal graph that underlies the SFM (Figure 2a) by separately simulating each edge of the graph as a multilayer perceptron. This allows us to simulate W and Y "naturally" (randomly sampling the protected attribute X) and in the counterfactual setting (forcibly setting X to 0 or 1 and simulating $W_{X_0}, W_{X_1}, Y_{X_0, W_{X_0}}, Y_{X_0, W_{X_1}}, Y_{X_1, W_{X_1}}$, and $Y_{X_1, W_{X_0}}$). This allows us to calculate the "true" natural direct effect (NDE), natural

indirect effect (NIE), and spurious effect (SE) as in [Plečko and Bareinboim \[2024\]](#). We select dimensions for simulation of W between $|W| = 750$ and $|W| = 1,750$, as this encapsulates the dimensionality of W in our selected tasks ($|W| = 768$ for AMI, SLE, and T2DM; $|W| = 1,570$ for SCZ). We select $|Z| = 10$ for $|W| = 750$ (again, to mimic the dimensionality of the AMI, SLE, and T2DM tasks) and $|Z| = 30$ for the other dimensions of W to mimic the SCZ task. The high error in NDE and NIE (Figure 9) motivate us to experiment with dimensionality reduction as a method for improving estimate accuracy.

Dim W	N	NDE Error (%)		NIE Error (%)		SE Error (%)	
		No Intervention	PFI (20%)	No Intervention	PFI (20%)	No Intervention	PFI (20%)
750	10,000	79.310 (4.081, 228.536)	45.571 (2.173, 128.103)	123.927 (10.276, 372.327)	78.161 (3.617, 213.691)	11.611 (2.075, 19.487)	11.611 (2.075, 19.487)
	50,000	39.337 (1.650, 106.857)	11.398 (0.218, 35.774)	64.421 (3.498, 181.584)	18.071 (0.975, 56.431)	6.670 (5.098, 8.307)	6.670 (5.098, 8.307)
	75,000	36.642 (1.972, 120.840)	12.232 (0.503, 34.469)	58.959 (3.372, 193.431)	19.884 (0.898, 55.653)	0.906 (0.044, 2.328)	0.906 (0.044, 2.328)
	100,000	32.274 (1.530, 103.406)	11.406 (0.937, 31.692)	52.526 (2.702, 167.299)	17.664 (1.282, 49.180)	1.004 (0.069, 2.220)	1.004 (0.069, 2.220)
1,000	10,000	40.091 (1.598, 111.827)	21.517 (0.881, 57.915)	69.529 (3.591, 193.792)	40.135 (2.423, 82.119)	12.248 (5.856, 17.251)	12.248 (5.856, 17.251)
	50,000	10.350 (0.508, 28.142)	13.499 (1.446, 29.392)	26.081 (1.064, 69.714)	29.869 (3.117, 70.365)	0.561 (0.035, 1.643)	0.561 (0.035, 1.643)
	75,000	13.032 (1.150, 38.663)	4.598 (0.242, 12.138)	31.584 (1.855, 96.201)	15.713 (2.189, 35.134)	1.148 (0.257, 2.121)	1.148 (0.257, 2.121)
	100,000	11.365 (0.251, 32.018)	4.355 (0.381, 11.531)	32.525 (3.196, 86.739)	18.105 (2.244, 36.530)	2.016 (1.047, 2.856)	2.016 (1.047, 2.856)
1,250	10,000	42.681 (2.086, 116.673)	24.080 (1.929, 53.761)	121.390 (6.251, 325.329)	64.552 (7.563, 141.625)	4.476 (0.289, 10.938)	4.476 (0.289, 10.938)
	50,000	22.106 (2.093, 40.526)	43.752 (30.457, 54.553)	39.915 (3.840, 87.147)	93.578 (58.198, 125.238)	7.433 (4.896, 10.168)	7.433 (4.896, 10.168)
	75,000	15.936 (2.587, 29.818)	33.401 (26.190, 40.575)	35.799 (1.166, 73.500)	83.999 (63.064, 105.462)	4.560 (2.724, 6.340)	4.560 (2.724, 6.340)
	100,000	10.053 (0.379, 25.939)	32.213 (26.405, 37.901)	29.930 (1.701, 78.364)	93.471 (77.614, 111.653)	1.233 (0.166, 2.716)	1.233 (0.166, 2.716)
1,500	10,000	35.332 (2.854, 89.697)	16.419 (1.197, 44.223)	106.558 (4.453, 255.723)	30.348 (1.525, 90.778)	41.912 (11.469, 70.110)	41.912 (11.469, 70.110)
	50,000	20.344 (2.301, 37.949)	6.178 (0.825, 15.590)	56.469 (8.808, 100.389)	10.657 (0.724, 31.218)	8.394 (0.553, 15.522)	8.394 (0.553, 15.522)
	75,000	12.428 (0.804, 26.085)	8.365 (2.351, 14.346)	32.814 (3.874, 64.966)	18.465 (4.110, 32.993)	3.927 (0.415, 11.430)	3.927 (0.415, 11.430)
	100,000	8.868 (0.287, 20.068)	9.830 (3.856, 15.062)	30.572 (1.641, 63.498)	13.857 (1.030, 27.395)	16.915 (11.021, 21.612)	16.915 (11.021, 21.612)
1,750	10,000	49.700 (1.787, 107.959)	20.749 (4.744, 40.926)	94.719 (4.689, 203.145)	35.255 (3.447, 74.458)	11.507 (3.299, 19.435)	11.507 (3.299, 19.435)
	50,000	20.712 (5.537, 35.845)	4.582 (0.098, 12.260)	42.497 (12.590, 72.629)	9.758 (0.382, 26.426)	2.327 (0.242, 4.805)	2.327 (0.242, 4.805)
	75,000	21.926 (11.099, 34.154)	6.467 (1.534, 13.016)	37.904 (16.668, 62.389)	7.129 (0.590, 18.568)	2.113 (0.541, 3.633)	2.113 (0.541, 3.633)
	100,000	26.314 (11.594, 38.866)	7.229 (1.439, 11.650)	50.649 (19.963, 77.349)	12.055 (1.772, 21.804)	1.485 (0.105, 2.852)	1.485 (0.105, 2.852)

Table 2: Comparison of NDE, NIE, and SE Errors across dimensions and sample sizes. Values shown are Mean percent error (95% CI). Note that SE is not expected to change, as the representation of W does not impact the spurious effect estimate. PFI (20%) refers to use of permutation feature analysis (PFI) to identify the top 20% of features most important for predicting the outcome Y ; this dimensionality reduction technique significantly improves the NDE and NIE estimation error in four out of the five experiments shown.

In addition to testing dimensionality reduction techniques for $|W| = 1,750$ (Figure 5), we test dimensionality reduction for $|W| = 750$, $|W| = 1,000$, $|W| = 1,250$, and $|W| = 1,500$ (Figure 11). Across three out of these four synthetic experiments, we find that dimensionality reduction conducted by selecting features important to learning the outcome model ("Learn Y ") are most effective lowering estimation error. This finding is consistent with the synthetic experiments for $|W| = 1,750$. In Table 2, we present the estimation error under no dimensionality reduction (No Intervention) and the best-performing intervention (using PFI to select the top 20% of important features for predicting Y).

11 Supplementary Methods

11.1 Tuning fairness parameters

In addition to the baseline model, we train models that implement the fairness interventions outlined in Section 4.5. In the cases where we train multiple models corresponding to one fairness intervention, we select the model with the best validation-set tradeoff between binary cross entropy loss (performance) and average causal effect (fairness).

For interventions that impose fairness constraints using a loss regularization term (**path-specific inprocessing, equalized odds**), the "fairness parameter" (λ) controls the strength of the loss regularization term relative to the binary cross entropy loss. A larger value for λ increases the scale of the loss regularization term; we vary λ logarithmically between 0.1 and 100. For interventions that use feature selection (**greedy feature selection, "unbiased" feature selection**), the "fairness parameter" controls the number of features used by the model. For AMI, SLE, and T2DM tasks (where the total dimensionality of $|W|$ is 768), we test *number of features* = 300, 400, 500, 600, 700. For SCZ (total dimensionality of features is $|W| = 1,570$), we test *number of features* = 400, 500, 550, 600. While this corresponds to a lower percentage of features relative to the non-SCZ tasks due to prior experiments that found that limiting the baseline SCZ model to the top 30% of features (471) does not diminish model performance. In the case of **causally fair resampling**, we test the impact of targeting the NDE only or the TE (NDE + NIE). This method does not allow for targeting of the SE. We only report the "better" model due to the similarity of the outputs across all clinical tasks.

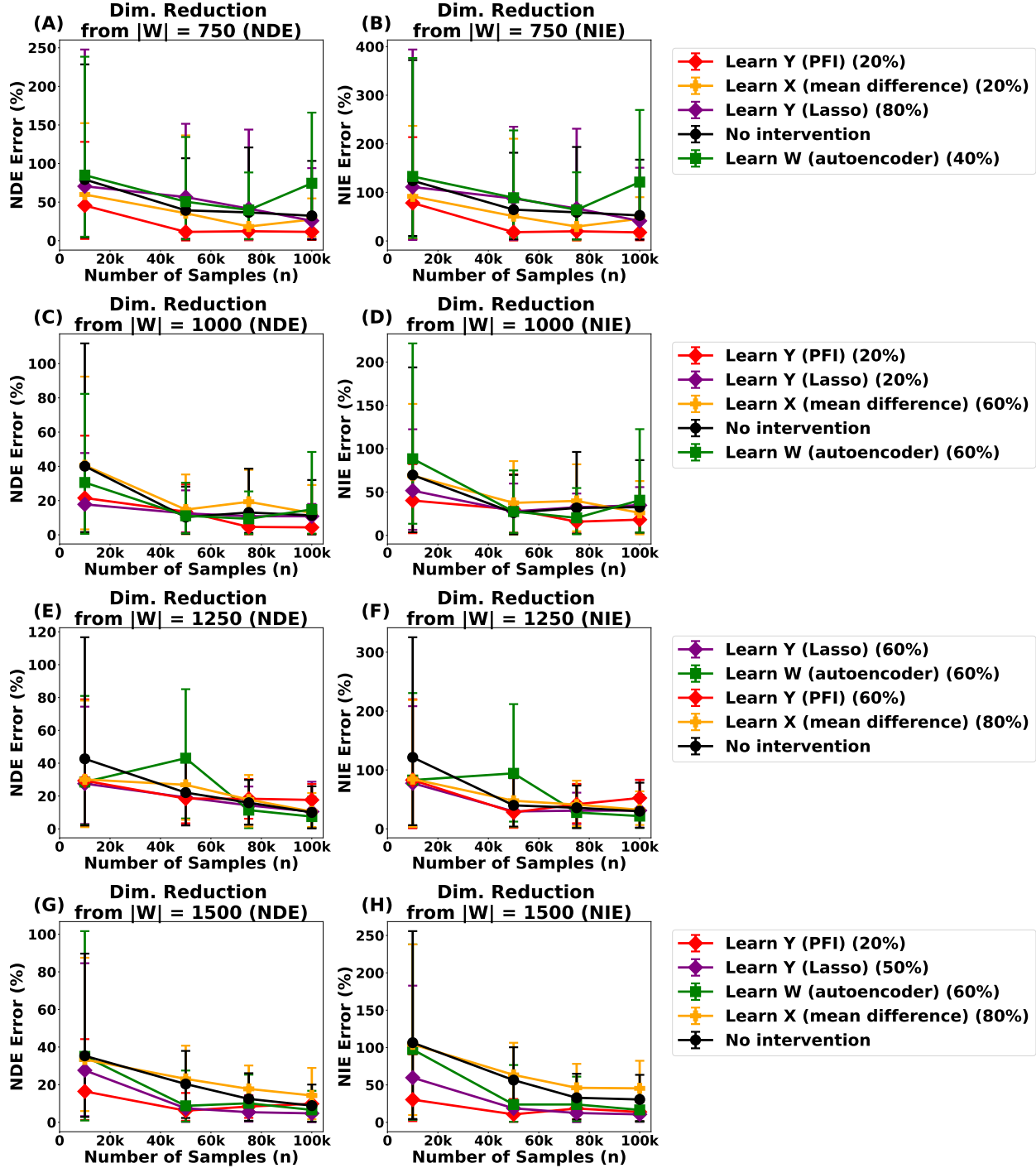


Figure 11: Error in the path-specific causal estimates for dimensionality $|W| < 1,750$. Each line corresponds to a different dimensionality reduction methods, with the black line corresponding to no dimensionality reduction. The NDE estimation error is reflected in (A), (C), (E), and (G) and the NIE estimation error is reflected in part (B), (D), (F), and (H). We find that interventions that identify features important for predicting the outcome (Y) generally outperform other methods.

Figure 12: This figure contains a set of 8 subplots – each row of two subplots visualizes the NDE and NIE error for a given dimension. Each plot is a line plot with colored lines corresponding to the dimensionality reduction method and associated error bars.

12 Additional Results: AMI

The "at-risk" cohort for developing AMI includes individuals with at least two years of observation who have a diagnostic code related to ischemic heart disease. Individuals remain in the cohort if they have had a previous AMI (as this is an acute event), as long as it was over 6 months prior to the prediction visit (to prevent label leakage). We present the tradeoffs between model performance and all path-specific effects in Figure 13 and observe the importance of prioritizing causal pathways based on domain knowledge: "unbiased" and greedy feature selection both slightly exacerbate the spurious effect (SE between -0.015 and -0.010) but demonstrate significant improvement in the NIE (0.021 and 0.068, respectively) relative to causally fair resampling, which eliminates the SE but retains a significantly higher NIE (0.107).

When we compare the correlations between the sensitive attribute and the (predicted or true) outputs in the models, we find a small positive correlation between male gender and the outcome in the data (Figure 15). This correlation is significantly stronger in the baseline model, and is reduced significantly by each of the three fairness intervention. The ranking of each of gender-prediction correlations over these fairness interventions corresponds to the ranking of NIE, with the highest magnitude NIE and correlations belonging to causally fair resampling, followed by greedy feature selection and then selection of "unbiased" features. All three interventions, however, lead to significantly lower correlation than exists in the baseline model.

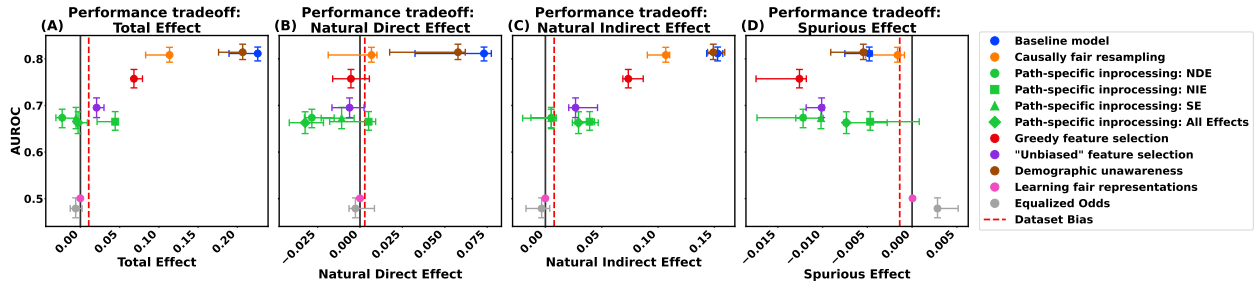


Figure 13: AMI: Tradeoff between model performance (AUROC) and path-specific causal effects for each of the tested interventions. Larger AUROC indicates better performance, and lower magnitude for TE (a), NDE (b), NIE (c), and SE (d) indicate a more "fair" model with respect to that specific causal pathway.

Figure 14: Set of four subplots with colored points and associated error bars. The x-axis corresponds to the path-specific causal effect and the y-axis corresponds to model performance. The points are colored based on the fairness intervention.

Experiment	AUROC	Calibration	TE	NDE	NIE	SE
Baseline model	0.812 (0.796, 0.825)	0.387 (0.387, 0.388)	0.226 (0.189, 0.226)	0.073 (0.032, 0.077)	0.153 (0.143, 0.157)	-0.005 (-0.008, -0.004)
Data	-	-	0.011 (0.005, 0.011)	0.003 (-0.003, 0.004)	0.008 (0.005, 0.009)	-0.001 (-0.001, -0.000)
Causally fair resampling	0.808 (0.793, 0.825)	0.011 (0.010, 0.012)	0.114 (0.083, 0.114)	0.007 (-0.019, 0.010)	0.107 (0.090, 0.110)	-0.002 (-0.005, -0.001)
Path-specific inprocessing: All Effects	0.663 (0.640, 0.686)	0.385 (0.385, 0.386)	-0.003 (-0.003, 0.009)	-0.032 (-0.042, -0.022)	0.029 (0.024, 0.047)	-0.007 (-0.008, -0.003)
Path-specific inprocessing: NDE	0.674 (0.652, 0.692)	0.389 (0.389, 0.390)	-0.023 (-0.031, -0.023)	-0.028 (-0.033, -0.015)	0.005 (-0.013, 0.009)	-0.012 (-0.017, -0.012)
Path-specific inprocessing: NIE	0.665 (0.647, 0.687)	0.384 (0.384, 0.384)	0.044 (0.021, 0.045)	0.005 (-0.018, 0.009)	0.039 (0.026, 0.044)	-0.005 (-0.005, 0.001)
Path-specific inprocessing: SE	0.673 (0.650, 0.696)	0.384 (0.384, 0.385)	-0.006 (-0.024, -0.005)	-0.011 (-0.023, -0.003)	0.005 (-0.020, 0.009)	-0.010 (-0.013, -0.010)
Greedy feature selection	0.757 (0.738, 0.777)	0.391 (0.391, 0.392)	0.068 (0.068, 0.079)	-0.005 (-0.016, 0.006)	0.074 (0.069, 0.087)	-0.013 (-0.017, -0.012)
"Unbiased" feature selection	0.695 (0.674, 0.716)	0.391 (0.390, 0.391)	0.021 (0.020, 0.030)	-0.006 (-0.017, 0.002)	0.027 (0.021, 0.046)	-0.010 (-0.012, -0.010)
Demographic unawareness	0.814 (0.799, 0.832)	0.389 (0.388, 0.390)	0.207 (0.176, 0.207)	0.058 (0.017, 0.062)	0.149 (0.144, 0.159)	-0.005 (-0.009, -0.005)
Learning fair representations	0.501 (0.500, 0.503)	0.011 (0.010, 0.012)	-0.000 (-0.000, 0.000)	0.000 (-0.000, 0.001)	-0.000 (-0.000, 0.000)	0.000 (-0.000, 0.000)
Equalized Odds	0.479 (0.459, 0.502)	0.384 (0.384, 0.385)	-0.006 (-0.013, 0.002)	-0.003 (-0.006, 0.009)	-0.003 (-0.017, 0.004)	0.003 (0.003, 0.005)

Table 3: AMI: Impact of fairness interventions on model performance and path-specific causal effects

13 Additional Results: SLE

The "at-risk" cohort for SLE comprises individuals with at least one symptom of SLE or one SLE-related prescription. We restrict prediction to the first occurrence of SLE due to its chronic nature. In addition to our findings that causally fair resampling and "unbiased" feature selection achieve the best NDE-performance tradeoff (Figure 17B), we find that path-specific inprocessing methods are able to more effectively control the NIE; however, this comes at a further reduction in model performance. The spurious effect is small (< 0.005) across all models.

When we examine correlation between patient gender and (predicted) outcome, we observe the lowest-magnitude correlation between gender and the outcome in the data and the largest correlation in the demographic-unaware model, which exhibited the largest NDE. Causally fair resampling renders the correlation between gender and predicted

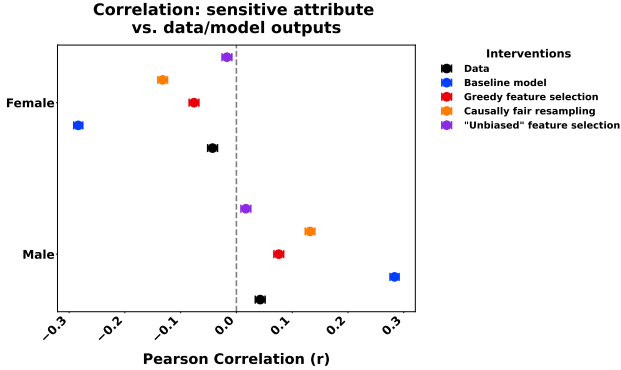


Figure 15: Correlation between patient gender and output. We visualize the correlation (Pearson R) between gender and the true output (Data), as well as between gender and the predicted output for the baseline model and best fairness interventions (causally fair resampling, greedy feature selection, "unbiased" feature selection).

Figure 16: Scatter plot with points colored based on the fairness intervention; the x-axis corresponds to Pearson Correlation, and the y-axis corresponds to the sensitive attribute (gender).

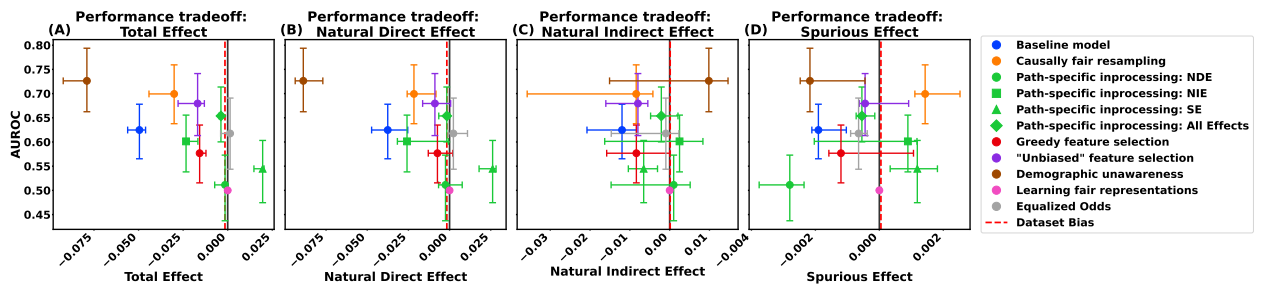


Figure 17: SLE: Tradeoff between model performance (AUROC) and path-specific causal effects for each of the tested interventions. Larger AUROC indicates better performance, and lower magnitude for TE (a), NDE (b), NIE (c), and SE (d) indicate a more "fair" model with respect to that specific causal pathway.

Figure 18: Set of four subplots with colored points and associated error bars. The x-axis corresponds to the path-specific causal effect and the y-axis corresponds to model performance. The points are colored based on the fairness intervention.

Table 4: SLE: Impact of fairness interventions on model performance and path-specific causal effects

Experiment	AUROC	Calibration	TE	NDE	NIE	SE
Baseline model	0.625 (0.565, 0.678)	0.253 (0.253, 0.253)	-0.050 (-0.056, -0.046)	-0.038 (-0.047, -0.025)	-0.012 (-0.021, -0.008)	-0.002 (-0.002, -0.001)
Data	-	-	-	-	0.000 (-0.000, 0.000)	0.000 (-0.000, 0.000)
Causally fair resampling	0.699 (0.638, 0.759)	0.001 (0.001, 0.002)	-0.030 (-0.044, -0.030)	-0.022 (-0.026, -0.008)	-0.008 (-0.036, -0.004)	0.001 (0.001, 0.003)
Path-specific inprocessing: All Effects	0.654 (0.600, 0.714)	0.253 (0.253, 0.253)	-0.004 (-0.005, -0.004)	-0.002 (-0.007, 0.000)	-0.002 (-0.005, 0.002)	-0.001 (-0.001, -0.000)
Path-specific inprocessing: NDE	0.511 (0.437, 0.573)	0.253 (0.253, 0.253)	-0.001 (-0.007, -0.001)	-0.002 (-0.007, 0.008)	0.001 (-0.015, 0.005)	-0.003 (-0.004, -0.002)
Path-specific inprocessing: NIE	0.601 (0.538, 0.656)	0.253 (0.253, 0.253)	-0.023 (-0.024, -0.017)	-0.026 (-0.032, -0.001)	0.002 (-0.016, 0.008)	0.001 (-0.002, 0.001)
Path-specific inprocessing: SE	0.545 (0.475, 0.603)	0.253 (0.253, 0.253)	0.020 (0.015, 0.020)	0.026 (0.018, 0.028)	-0.007 (-0.010, -0.003)	0.001 (0.000, 0.002)
"Unbiased" feature selection	0.680 (0.613, 0.741)	0.253 (0.253, 0.253)	-0.017 (-0.028, -0.013)	-0.009 (-0.016, 0.001)	-0.008 (-0.016, -0.005)	-0.000 (-0.001, 0.001)
Greedy feature selection	0.577 (0.516, 0.635)	0.253 (0.253, 0.253)	-0.016 (-0.016, -0.012)	-0.007 (-0.013, 0.002)	-0.008 (-0.016, 0.000)	-0.001 (-0.002, 0.001)
Demographic unawareness	0.726 (0.662, 0.794)	0.253 (0.253, 0.253)	-0.079 (-0.092, -0.079)	-0.089 (-0.094, -0.077)	0.010 (-0.015, 0.015)	-0.002 (-0.002, -0.000)
Learning fair representations	0.500 (0.500, 0.500)	0.001 (0.001, 0.002)	-0.000 (-0.000, 0.000)	-0.000 (-0.000, 0.000)	0.000 (-0.000, 0.000)	0.000 (-0.000, 0.000)
Equalized Odds	0.618 (0.544, 0.691)	0.253 (0.253, 0.253)	0.001 (-0.004, 0.002)	0.002 (-0.001, 0.011)	-0.001 (-0.015, 0.002)	-0.001 (-0.001, -0.000)

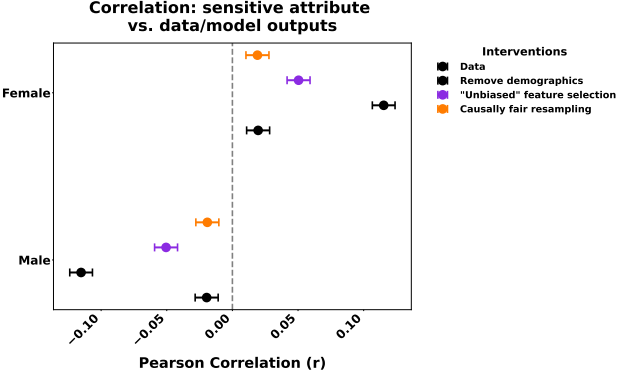


Figure 19: Correlation between patient gender and output. We visualize the correlation (Pearson R) between gender and the true output (Data), as well as between gender and the predicted output for the best-performing model (demographic unawareness) and best fairness interventions (causally fair resampling, "unbiased" feature selection).

Figure 20: Scatter plot with points colored based on the fairness intervention; the x-axis corresponds to Pearson Correlation, and the y-axis corresponds to the sensitive attribute (gender).

outcome equal to that in the data, while "unbiased" feature selection demonstrates a slightly larger magnitude of correlation relative to the data (Figure 19).

14 Additional Results: T2DM

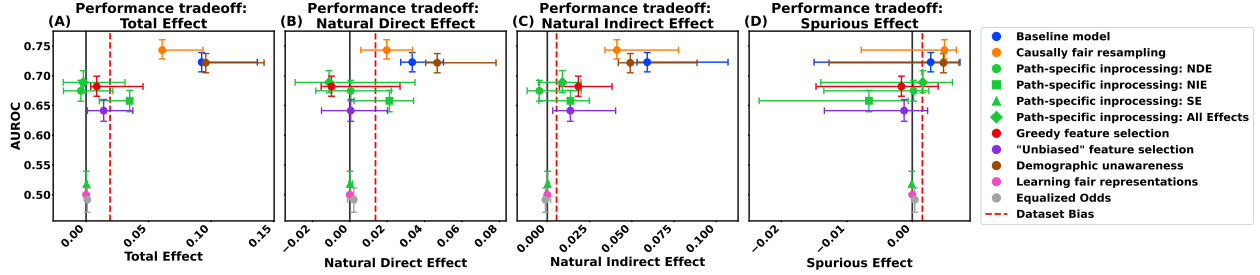


Figure 21: T2DM: Tradeoff between model performance (AUROC) and path-specific causal effects for each of the tested interventions. Larger AUROC indicates better performance, and lower magnitude for TE (a), NDE (b), NIE (c), and SE (d) indicate a more "fair" model with respect to that specific causal pathway.

Figure 22: Set of four subplots with colored points and associated error bars. The x-axis corresponds to the path-specific causal effect and the y-axis corresponds to model performance. The points are colored based on the fairness intervention.

Table 5: T2DM: Impact of fairness interventions on model performance and path-specific causal effects

Experiment	AUROC	Calibration	TE	NDE	NIE	SE
Baseline model	0.723 (0.706, 0.739)	0.388 (0.387, 0.388)	0.092 (0.092, 0.137)	0.033 (0.027, 0.050)	0.059 (0.053, 0.107)	0.003 (-0.015, 0.007)
Data	-	-	0.019 (0.003, 0.019)	0.014 (0.002, 0.016)	0.005 (-0.004, 0.007)	0.002 (0.000, 0.002)
Causally fair resampling	0.743 (0.728, 0.760)	0.017 (0.016, 0.018)	0.061 (0.060, 0.093)	0.020 (0.006, 0.034)	0.041 (0.034, 0.078)	0.005 (-0.008, 0.007)
Path-specific inprocessing: All Effects	0.689 (0.671, 0.709)	0.387 (0.387, 0.388)	-0.002 (-0.018, 0.031)	-0.011 (-0.029, 0.035)	0.009 (-0.005, 0.020)	0.002 (-0.014, 0.006)
Path-specific inprocessing: NDE	0.675 (0.657, 0.692)	0.379 (0.378, 0.379)	-0.004 (-0.018, 0.021)	0.001 (-0.018, 0.022)	-0.005 (-0.012, 0.020)	0.000 (-0.014, 0.003)
Path-specific inprocessing: NIE	0.658 (0.639, 0.675)	0.382 (0.382, 0.383)	0.035 (0.011, 0.035)	0.021 (0.002, 0.034)	0.014 (-0.005, 0.025)	-0.007 (-0.023, -0.001)
Path-specific inprocessing: SE	0.518 (0.501, 0.539)	0.378 (0.378, 0.378)	0.000 (0.000, 0.001)	0.000 (-0.000, 0.001)	0.000 (-0.000, 0.001)	-0.000 (-0.000, -0.000)
Greedy feature selection	0.682 (0.666, 0.699)	0.379 (0.379, 0.380)	0.009 (0.004, 0.046)	-0.010 (-0.015, 0.027)	0.018 (0.007, 0.038)	-0.002 (-0.015, 0.004)
"Unbiased" feature selection	0.641 (0.623, 0.660)	0.383 (0.383, 0.384)	0.014 (0.001, 0.037)	0.000 (-0.015, 0.020)	0.014 (0.003, 0.040)	-0.001 (-0.013, 0.002)
Demographic unawareness	0.722 (0.705, 0.737)	0.387 (0.386, 0.388)	0.096 (0.095, 0.142)	0.047 (0.041, 0.078)	0.049 (0.042, 0.089)	0.005 (-0.013, 0.007)
Learning fair representations	0.500 (0.500, 0.500)	0.017 (0.016, 0.018)	-0.000 (-0.000, 0.000)	-0.000 (-0.000, 0.000)	0.000 (-0.000, 0.000)	0.000 (-0.000, 0.000)
Equalized Odds	0.492 (0.470, 0.511)	0.382 (0.381, 0.382)	0.001 (0.001, 0.002)	0.002 (-0.001, 0.003)	-0.001 (-0.002, 0.002)	0.000 (-0.000, 0.000)

We use a validated diabetes phenotype definition [Suchard et al., 2021] to identify individuals from our "at risk" cohort who go on to develop T2DM. Prediction is restricted to the first diagnosis of T2DM due to its chronic nature. Beyond the NDE-NIE-performance tradeoff discussed in Section 5.5, we find that the spurious effect is insignificant in the

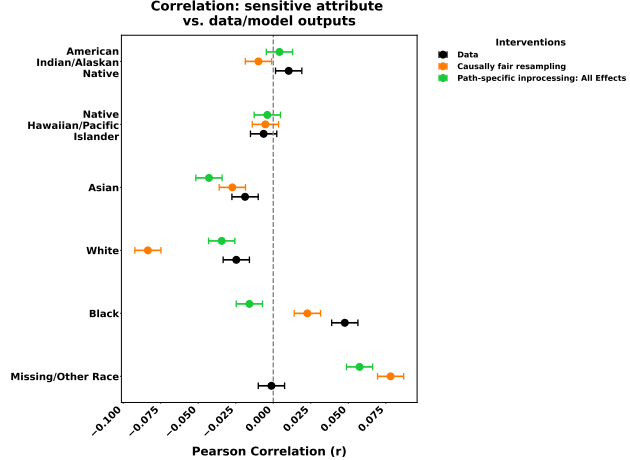


Figure 23: Correlation between patient race and output. We visualize the correlation (Pearson R) between race and the true output (Data), as well as between race and the predicted output for the best-performing model (causally fair resampling) and best fairness interventions (path-specific inprocessing: all effects).

Figure 24: Scatter plot with points colored based on the fairness intervention; the x-axis corresponds to Pearson Correlation, and the y-axis corresponds to the sensitive attribute (race).

baseline model and across all fairness interventions (Figure 21D). We now examine the correlation between the sensitive attribute (race) and true/predict outcome across the data and models (Figure 23). For White individuals, the causally fair resampling intervention (highest performance, largest NDE and NIE) demonstrates a strong negative correlation between race and predicted outcome. The data and the path-specific in-processing intervention (lower performance, insignificant NDE and NIE) demonstrate lower-magnitude negative correlations. For Black individuals, both the causally fair resampling model and the path-specific in-processing model are associated with lower-magnitude correlations between race and predicted output compared to the raw data; however, this correlation is positive for causally fair resampling (0.023, [0.014, 0.031]) and negative for path-specific in-processing (-0.016, [-0.025, -0.007]). For American Indian/Alaskan Native and Native Hawaiian/Pacific Islander individuals, the correlations are similarly small in the data and both models. There is a negative correlation between race and T2DM for Asian individuals, but this correlation is again similar across the data and both models. For individuals with race recorded as Missing/Other, we find no correlation between race and T2DM in the data, but a significant positive correlation in both models; this correlation is stronger under the causally fair resampling intervention.

15 Additional Results: SCZ

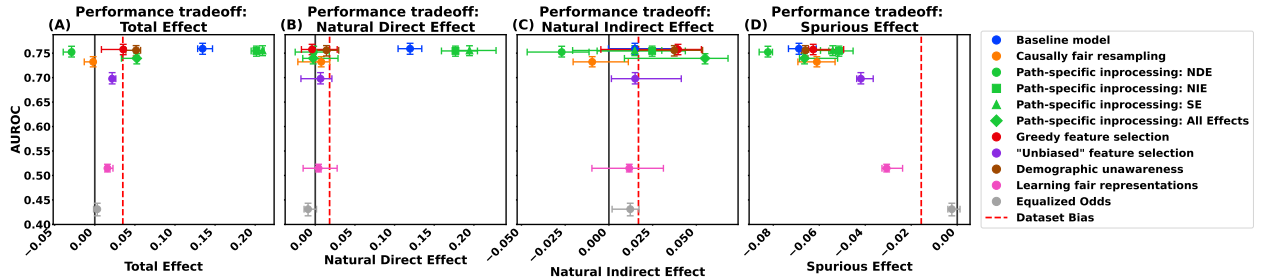


Figure 25: SCZ: Tradeoff between model performance (AUROC) and path-specific causal effects for each of the tested interventions. Larger AUROC indicates better performance, and lower magnitude for TE (a), NDE (b), NIE (c), and SE (d) indicate a more "fair" model with respect to that specific causal pathway.

Figure 26: Set of four subplots with colored points and associated error bars. The x-axis corresponds to the path-specific causal effect and the y-axis corresponds to model performance. The points are colored based on the fairness intervention.

Table 6: SCZ: Impact of fairness interventions on model performance and path-specific causal effects

Experiment	AUROC	Calibration	TE	NDE	NIE	SE
Baseline model	0.759 (0.748, 0.770)	0.065 (0.063, 0.068)	0.134 (0.128, 0.147)	0.120 (0.104, 0.134)	0.015 (-0.000, 0.039)	-0.069 (-0.073, -0.061)
Data	-	-	0.035 (0.029, 0.036)	0.018 (0.005, 0.031)	0.017 (0.003, 0.027)	-0.016 (-0.017, -0.012)
Causally fair resampling	0.732 (0.722, 0.743)	0.066 (0.064, 0.069)	-0.002 (-0.013, 0.001)	0.008 (-0.022, 0.018)	-0.010 (-0.020, 0.011)	-0.061 (-0.069, -0.053)
Path-specific inprocessing: All Effects	0.739 (0.728, 0.749)	0.066 (0.064, 0.069)	0.052 (0.033, 0.055)	-0.003 (-0.016, 0.029)	0.055 (0.009, 0.068)	-0.066 (-0.069, -0.052)
Path-specific inprocessing: NDE	0.752 (0.742, 0.764)	0.067 (0.064, 0.069)	-0.029 (-0.039, -0.027)	-0.002 (-0.025, 0.018)	-0.027 (-0.047, -0.011)	-0.082 (-0.086, -0.080)
Path-specific inprocessing: NIE	0.755 (0.744, 0.764)	0.066 (0.063, 0.068)	0.202 (0.195, 0.204)	0.177 (0.159, 0.204)	0.025 (-0.007, 0.044)	-0.051 (-0.056, -0.045)
Path-specific inprocessing: SE	0.755 (0.745, 0.765)	0.066 (0.063, 0.068)	0.209 (0.203, 0.211)	0.194 (0.179, 0.228)	0.015 (-0.021, 0.030)	-0.054 (-0.059, -0.050)
Greedy feature selection	0.758 (0.747, 0.768)	0.065 (0.063, 0.068)	0.035 (0.008, 0.037)	-0.004 (-0.017, 0.028)	0.040 (-0.005, 0.053)	-0.063 (-0.065, -0.049)
"Unbiased" feature selection	0.698 (0.687, 0.710)	0.068 (0.065, 0.070)	0.022 (0.020, 0.026)	0.007 (-0.018, 0.021)	0.015 (0.001, 0.041)	-0.042 (-0.044, -0.037)
Demographic unawareness	0.756 (0.744, 0.765)	0.065 (0.063, 0.068)	0.052 (0.039, 0.057)	0.014 (-0.004, 0.030)	0.037 (0.016, 0.054)	-0.066 (-0.068, -0.051)
Learning fair representations	0.515 (0.507, 0.523)	0.071 (0.069, 0.074)	0.016 (0.014, 0.023)	0.004 (-0.015, 0.028)	0.012 (-0.010, 0.031)	-0.031 (-0.033, -0.024)
Equalized Odds	0.431 (0.417, 0.443)	0.071 (0.069, 0.074)	0.003 (-0.002, 0.004)	-0.009 (-0.014, 0.002)	0.012 (0.002, 0.017)	-0.002 (-0.004, 0.001)

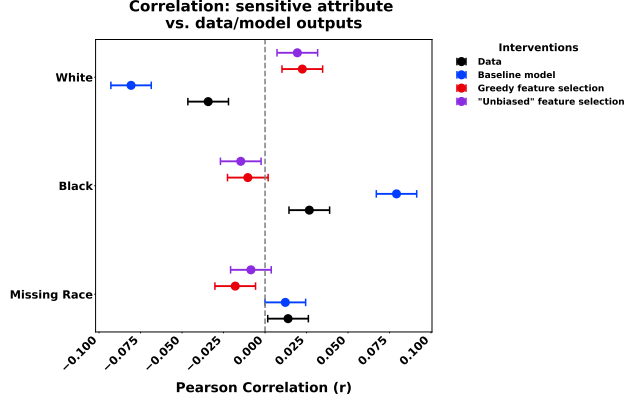


Figure 27: Correlation between patient race and output. We visualize the correlation (Pearson R) between race and the true output (Data), as well as between race and the predicted output for the baseline model and best fairness interventions (greedy feature selection, "unbiased" feature selection).

Figure 28: Scatter plot with points colored based on the fairness intervention; the x-axis corresponds to Pearson Correlation, and the y-axis corresponds to the sensitive attribute (race).

We define our schizophrenia cohort as individuals with at least two SCZ diagnoses and three years of observation prior to the first diagnosis, as validated in [Finnerty et al. \[2024\]](#). We made our prediction (any future diagnosis of SCZ) one year after an individual's first psychosis diagnosis and removed individuals who were diagnosed with SCZ within one year of their initial psychosis diagnosis. We focus on SCZ prediction in the MDCD dataset because there is not sufficient power for these analyses in the CUMC-EHR dataset. When we perform fairness interventions on the schizophrenia model, we observe clear tradeoffs between fairness with respect to the NDE and the NIE: demographic awareness and greedy feature selection both significantly reduce the NDE, but they increase the NIE (Figure 25). When we examine the correlation between race and true/predicted output (Figure 27), the baseline model exacerbates this correlation relative to the data for Black and White patients. Both the greedy feature selection and "unbiased" feature selection result in similar correlations, which lower the magnitude of the correlation to the level found in the data. For patients with missing race, the correlation between race and output is similar in the data and baseline model and is reversed, although similar in magnitude in both the "fairer" models. All correlations between "Missing" race and SCZ output are small (< 0.015).